

THREE DIMENSIONAL ANALYSIS OF LATERAL EXTRUSION OF SOME COMPLEX FORMS

A THESIS SUBMITTED IN PARTIAL FULFILMENT OF THE
REQUIREMENTS FOR THE DEGREE OF

Master of Technology
in
Mechanical Engineering

By

Sanjeeb Kumar Tirkey



Department of Mechanical Engineering
National Institute of Technology
Rourkela

MAY, 2007

THREE DIMENSIONAL ANALYSIS OF LATERAL EXTRUSION OF SOME COMPLEX FORMS

A THESIS SUBMITTED IN PARTIAL FULFILMENT OF THE
REQUIREMENTS FOR THE DEGREE OF

**Master of Technology
in
Mechanical Engineering**

[Specialization: Production Engineering]

By

Sanjeeb Kumar Tirkey

Under the Guidance of

Dr. Susanta Kumar Sahoo

Department of Mechanical Engineering



**Department of Mechanical Engineering
National Institute of Technology
Rourkela**

May, 2007



National Institute of Technology Rourkela

CERTIFICATE

This is to certify that the thesis entitled “**Three Dimensional Analysis of Lateral Extrusion Of Some Complex Forms**” submitted by **Sri Sanjeeb Kumar Tirkey** in partial fulfillment of the requirements for the award of Master of Technology degree in Mechanical Engineering with specialization in Production Engineering to the National Institute of Technology, Rourkela (Deemed University) is an authentic work carried out by him under my supervision and guidance.

To the best of my knowledge, the matter embodied in the thesis has not been submitted to any other University / Institute for the award of any Degree or Diploma.

Dr. Susanta Kumar Sahoo
Dept. of Mechanical Engg.
National Institute of Technology
Rourkela 769008

ACKNOWLEDGEMENT

I avail this opportunity to extend my hearty indebtedness to my guide **Dr.S.K.Sahoo**, Asst.Professor, Mechanical Engineering for his valuable guidance constant encouragement and kind help at different stages for the execution of this dissertation work.

I am extremely thankful to **Prof. B. K. Nanda**, Head, Department of Mechanical Engineering and **Prof. K. P. Maity**, Course Coordinator for their help and advice during the course of this work.

I am also thankful to **Mr.K.Nayak**, Technical assistant, Mechanical Engg. and **Mr.Y.Ali**, Technical assistant of central workshop for their help during the execution of experiment.

My friends and class mates **Sri Nagamahendra Babu** and **M.Chaithanya** deserve my special thanks for their help and support throughout this work.

I am also thankful to all my well wishers, class mates and friends for their inspiration and help.

Date:

Sanjeeb Kumar Tirkey
Roll No. 20503042

CONTENTS

Chapter 1	Introduction	1-17
Chapter 2	Literature Review	18-20
Chapter 3	Theoretical Analysis	21-26
Chapter 4	Experimental Investigation	27-42
Chapter 5	Application of the ALGOR Software	43-52
Chapter 6	Results & Discussion	53-55
Chapter 7	Conclusions & Future Recommendations	56
	References	57-58

ABSTRACT

An upper bound solution for lateral extrusion of square, hexagon, spline and tracoidal forms has been developed. A simple kinematically admissible velocity field with optimization parameter is proposed. From the proposed velocity field the upper bound solution on relative punch pressure and extrusion load are determined with respect to chosen process parameters. The results are compared with theoretical and experimental result from a reference to illustrate the validity of the proposed velocity fields. This is indicating that the analysis presented here renders better upper bound solution.

Three-dimensional brick shaped elements are utilized in finite element analysis by ALGOR software with linear and non-linear metal applied to upset forging of L shaped blocks. The upper bound elemental technique also used to analyze the problem. Detailed formulations of models are presented. The predictions both in forging load and the deformed configuration are in good agreement with the experiment qualitatively under different lubrication conditions.

The proposed velocity field gives higher load values than the values experimentally obtained within 25 percent. The velocity field proposed in the present investigation can be used conveniently with short computational time for the prediction of extrusion loads & deformations in heading of different shapes. A higher order polynomial velocity field can be tested to get better results for different section.

LIST OF FIGURES

FIGURE NO	FIGURE TITLE	PAGE NO
Fig.1.1	Classification of plastic-forming processes on the basis of compressive stress	7
Fig.1.2	Classification of plastic-forming processes on the basis of tension, tension and compression, bending, shear, torsion stresses	8
Fig.1.3	Classification of stress	9
Fig.1.4 (a)	classification of forming operation	9
Fig.1.4 (b)	classification of forming operation	10
Fig. 1.5	forward extrusion	11
Fig. 1.6	backward extrusion	11
Fig. 1.7	Lateral extrusion or radial extrusion	11
Fig. 1.8	Combination of backward and forward extrusion	12
Fig. 3.1	Lateral Extrusion for spline with four teeth	23
Fig 4.1	stress strain characteristics of Lead in compression test	29
Fig. 4.2	Theoretical calibration curve for standard ring 6:3:2	30
Fig. 4.3	Assembled Setup	31
Fig. 4.4	Explored Drawing of Assembled Setup	31
Fig. 4.5	Different Parts of the Setup	32
Fig. 4.6	Dimension. of punch or ram	33
Fig. 4.7	Dimension of die	34
Fig. 4.8	Dimension of die holder	34
Fig. 4.9	Dimension of container	35
Fig. 4.10	Dimension of square product	36
Fig. 4.11	Dimension of hexagon product	36

Fig. 4.12	Dimension of spline product	37
Fig. 4.13	Dimension of tracoidal product	37
Fig. 4.14	Experimental Setup on UTM	38
Fig. 4.15	Experimental Setup on UTM (close view)	39
Fig. 4.16	Photographs of Products (Square head)	39
Fig. 4.17	Photographs of Products (Hexagonal head)	39
Fig. 4.18	Photographs of Products (Tracoidal head)	40
Fig. 4.19	Photographs of Products (Spline head)	40
Fig. 4.20	Photographs of Products (Spline head) with Different Load	40
Fig. 4.21	Variation of extrusion pressure with stroke (Square head)	41
Fig. 4.22	Variation of extrusion pressure with stroke (Hexagonal head)	41
Fig. 4.23	Variation of extrusion pressure with stroke (Tracoidal head)	42
Fig. 4.24	Variation of extrusion pressure with stroke (Spline head)	42
Fig.5.1	Lager Analysis of square Product with 15 mm head	48
Fig.5.2	Lager Analysis of square Product with 14 mm head	48
Fig.5.3	Lager Analysis of square Product with 13 mm head	48
Fig.5.4	Lager Analysis of square Product with 12 mm head	48
Fig.5.5	Lager Analysis of square Product with 11 mm head	48
Fig.5.6	Lager Analysis of hexagon Product with 15 mm head	49
Fig.5.7	Lager Analysis of hexagon Product with 14 mm head	49
Fig.5.8	Lager Analysis of hexagon Product with 13 mm head	49
Fig.5.9	Lager Analysis of hexagon Product with 12 mm head	49
Fig.5.10	Lager Analysis of hexagon Product with 11 mm head	49
Fig.5.11	Lager Analysis of spline Product with 15 mm head	50

Fig.5.12	Lager Analysis of spline Product with 14 mm head	50
Fig.5.13	Lager Analysis of spline Product with 13 mm head	50
Fig.5.14	Lager Analysis of spline Product with 12 mm head	50
Fig.5.15	Lager Analysis of spline Product with 11 mm head	50
Fig.5.16	Lager Analysis of tracoidal Product with 15 mm head	51
Fig.5.17	Lager Analysis of tracoidal Product with 14 mm head	51
Fig.5.18	Lager Analysis of tracoidal Product with 13 mm head	51
Fig.5.19	Lager Analysis of tracoidal Product with 12 mm head	51
Fig.5.20	Lager Analysis of tracoidal Product with 11 mm head	51
Fig. 6.1	Variation of extrusion pressure with h/r_p (Square head)	54
Fig. 6.2	Variation of extrusion pressure with h/r_p (hexagonal head)	54
Fig. 6.3	Variation of extrusion pressure with h/r_p (Tracoidal head)	55
Fig. 6.4	Variation of extrusion pressure with h/r_p (Spline head)	55

NOMENCLATURE

h = maximum thickness of the head

r_0 = maximum diameter of the head without spline

R = maximum diameter of the head with spline

r_p = diameter of the billet or container

λ = is a multiplying factor (one of the optimizing parameter) with height of head, which separate the rigid region with deforming zone.

b, c, d, e = optimizing parameters

r, θ, z = axis of the cylindrical coordinate system

α = angle made by one symmetrical part (zone of consideration) at center

β = angle made by one half of the spline at center

J^* = total power consumption

W_i = internal power of deformation

W_s = power expended at the surfaces of velocity discontinuities between the elements

W_f = power utilized to overcome frictional resistance at billet-die interfaces.

P_{av} = is the average extrusion pressure

A = cross sectional area of the billet

U_o = is the ram velocity

$\frac{P_{av}}{\sigma_o}$ = the non-dimensional forging pressure

r, θ, z = The center of cylindrical coordinate, s taken at the center of the bottom surface.

Chapter 1

INTRODUCTION

INTRODUCTION

Extrusion is an often-used forming process among the different metal forming operations and its industrial history dates back to the 18th century. A billet is placed in the container and pressed by the punch, causing the metal to flow through a die with an opening. The process is basically classified into three categories according to the flow direction in relation to the punch movement. This classification is namely forward, backward and lateral extrusion. Metal flows in forward extrusion is the same as that of punch, while metal flows in opposite direction of the punch in backward extrusion. In lateral extrusion, metal flows perpendicular to the punch direction.

The research work for lateral extrusion is not as plenty as for forward and backward extrusion. Complex part such as collar flange, splines, trapezoidal, hexagonal, spur gear forms with a shaft are a few example of the product produced by lateral extrusion.

Spur gear and splines are some machine element mostly used to transmit load and torque by rotating generally at high speeds. There for there an industrial demand to produced these parts with high strength within narrow tolerances. It is known that plastically deformed gears have longer lifetime and higher fatigue strength when compared to machined gear made from the same material. Also metal forming offers a considerable amount of material saving when compared to machining. In order to reduced the plastically deformed products and become more competitive in a demanding industry, the forming must be performed to near net or net shaped parts to reduce the subsequent operations such as machining. Plank has been investigated the cold extrusion of gear like elements using a simple velocity field. The estimated load using their theoretical analysis is approximately 20% higher than their experimental load values when using aluminum. This discrepancy may be attributed to a simplified velocity field using in their calculations.

More than ten years ago, researchers started to be attracted by three-dimensional problems in metal forming. Today three-dimensional modeling is still regarded as a highlighted and

difficult problem. Different methods of analysis have been extended to three dimensional, among which the finite element analysis is most commonly used. Most of the results that have been published on three dimensional finite element method simulations are based on different software package like DEFORM-3D (ALGOR), FORGE-3.

Metal forming

With the rapid advancement of new technologies like aerospace, aircraft, missile and automobile, the need for light and high strength, anti corrosion products are observed. Now a day the main constrain is the amount material resources, which is depleting at an alarming rate. So considering all the aspects, industries mostly depend on metal forming operations to minimize the material losses. The advantages of metal forming processes are

- ❖ The desired size and shape are obtained through the plastic deformation of material.
- ❖ It's a very economical process where the desired size, shape and surface finish can be obtained without any significance loss of material.
- ❖ The input energy can be fruitfully utilized in improving the strength.
- ❖ Strain and hardness are increased due to strain hardening.

Forming

Forging is defined as the plastic deformation of a billet between tools (dies) to obtain the final configuration. It may be classified roughly into five categories: mechanical working , such as forging, extrusion rolling , drawing, and various sheet forming process; casting; powder and fiber metal forming; and joining process. Forming is generally employed for those components, which require high strength, high resistance to shock and vibration, and uniform properties. The tolerance provided on forging, are related to the weight of the forging. For heavier forging, more wide tolerances are provided.

- ❖ Forging have high strength and offer great resistance to impact and fatigue loads.
- ❖ It improves the grain structure of material and hence its mechanical properties.
- ❖ Because of intense working of flaws are seldom found and work piece has high reliability.
- ❖ Forging renders the parts uniform in density as well as dimension.

Forging is generally employed for those components, which require high strength, resistance to shock, vibration and uniform properties, and uniform densities.

Classification of metal forming

According to Altan

Metal forming processes are usually classified according to two broad categories:

- Bulk or massive forming
- Sheet forming

In both types of process, the surface of the deforming metal and the tools are in contact, and friction between them may have a major influence on material flow.

Bulk forming

In bulk forming, the input material is in billet, rod, or slab form and the surface-to-volume ratio in the formed part increases considerably under the action of largely compressive Loading.

Features

The deforming material, or work piece, undergoes large plastic (permanent) deformation, resulting in an appreciable change in shape or cross section. The portion of the work piece undergoing plastic deformation is genera than the portion undergoing elastic deformation; therefore, elastic deformation is negligible. much larger recovery after. Major **examples** of bulk forming operations are extrusion, forging, rolling, and drawing.

Sheet forming

In sheet forming, a piece of sheet metal is plastically deformed by tensile loads into a three-dimensional shape, often without significant changes in sheet thickness or surface characteristics.

Features

The work piece is a sheet or a part fabricated from a sheet. The deformation usually causes significant changes in the shape, but not the cross-sectional area, of the sheet. In some cases, the magnitudes of the plastic and the elastic deformations are Comparable; therefore, elastic recovery or spring back may be significant.

Examples are deep drawing, bending, and rubber pad forming.

According to Bouglar

Bouglar **has** classified metal forming operations or processes as follows:

According to the types of workpiece

Massive or bulk forming processes- the starting material is in form of semi finished Shapes, bars, etc; the work piece has a small surface to volume ratio; forming causes large changes in shape and cross section; the elastic recovery is usually negligible.

Sheet metal processes- the starting material is rolled sheet; the work piece has a large surface to volume ratio; forming causes large changes in shape but small changes in thickness; the elastic recovery is usually significant.

According to the effect of deformation and temperature on mechanical properties

- Hot working- dynamic recovery occurs, no strain hardening, deformation temperature range is $0.7 < T_M < 0.8$
where T_M = incipient melting temperature.
- Warm working- some strain hardening and/or precipitation hardening may occur, deformation temperature range is $0.3 < T_M < 0.5$.
- Cold working- strain hardening occurs, deformation temperature range is $< 0.3 T_M$.

According to the mode of deformation

- steady state- continuous wire drawing,
- non-steady state- die forging, and
- Mked or transitory- extrusion.

According to the system imposed on the work-piece

- Compression
- Tension
- Tension And Compression
- Bending
- Torsion
- Shear

According to Thomsen, Yang, and Kobayashi

According to Thomsen, Yang & Kobayashi **the** sheet metal operations in which plastic deformation is the principle mechanism causing changes of shape are given as:

a. squeezing

- Closed die forging
- Coining
- Upsetting (open dies)
- Upsetting (closed dies)
- Extruding flats and rounds
- Extruding hollow shapes
- Rolling
- Spin forging
- Spin forging of cones
- Swaging
- Kneeding
- Peening

b. Drawing

- Wire and bar drawing
- Tube drawing
- Deep drawing
- Embossing
- Stretching
- Bulging
- Roll forming
- Ironing

c. Bending

- Straight flanging
- Sketch flanging
- Shrink flanging
- Seaming

d. Cutting

- Press shearing
- Shaving
- Notching and nibbling
- Machining
- Piercing (i.e. lancing and perforating)
- Grinding (i.e. lapping, honing, polishing)
- Trimming
- Blanking

According to Kienzle

One of the main systems for the classification of the plastic- deformation processes on the basis of a stress system is the one presented by Kienzle who classified the processes on the basis of six types of stress systems as shown in Figure 1.1 and Figure 1.2.


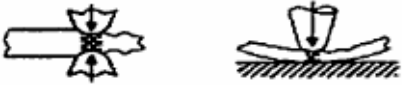





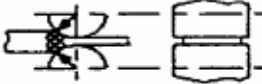


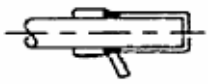
Mode	Process		
Compression	1	Upsetting	
	2	Drawing out	
	3	Drop forging coining	
	4	Pressing in closed die	
	5	Extrusion	
	6	Reducing	
	7	Swaging	
	8	Rolling	
	9	Reducer rolling	
	10	Spinning (conventional)	
	11	Power spinning	

Figure 1.1 Classification of plastic-forming processes on the basis of compressive stress













Mode	Process		
Tension	12	Expanding	
	13	Stretch forming	
	14	Embossing	
Tension and compression	15	Wire drawing	
	16	Deep drawing With blank-holder	
		Without blank-holder	
	17	Ironing	
Bending	18	At straight axis	
	19	At curved axis	
Shear	20	Shear spinning	
		Shear pressing	
Torsion	21	Setting	

Figure 1.2 Classification of plastic-forming processes on the basis of tension, tension and compression, bending, shear, torsion stresses

Classification of state of stress:

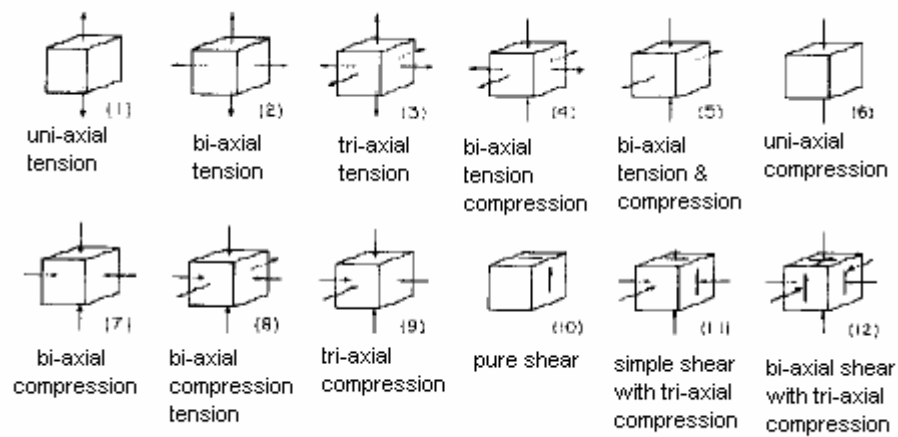


Fig. 1.3 Classification of stress

Classification of forming operation

sl no	processes	schematic diagram	state of stress in main part
1	rolling		7
2	forging		9
3	extruding		9
4	shear spinning		12

Fig. 1.4 (a) classification of forming operation

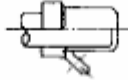
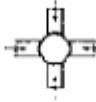
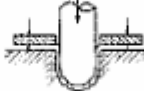
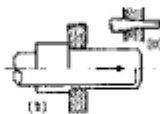


sl no	process	schematic diagram	state of stress in the main part
5	tube spinning		9
6	swaging or kneading		7
7	deep drawing		5
8	wire & tube drawing		8
9	stretching		2
10	straight bending		2 & 7
11	contoured flanging	(a) Contour	6, 2 & 7
		(b) Contour	1, 2 & 7

Fig. 1.4 (b) classification of forming operation

Extrusion

The forcing of solid metal through a suitably shaped orifice under compressive forces. Extrusion is somewhat analogous to squeezing toothpaste through a tube, although some cold extrusion processes more nearly resemble forging, which also deforms metals by application of compressive forces. Most metals can be extruded, although the process may not be economically feasible for high-strength alloys.

The most widely used method for producing extruded shapes is the direct, hot extrusion process. In this process, a heated billet of metal is placed in a cylindrical chamber and then compressed by a hydraulically operated ram.

The extrusion of cold metal is variously termed cold pressing, cold forging, cold extrusion forging, extrusion pressing, and impact extrusion. The term cold extrusion has become popular in the steel fabrication industry, while impact extrusion is more widely used in the nonferrous field.

Advantages of cold extrusion are higher strength because of severe strain-hardening, good finish and dimensional accuracy, and economy due to fewer operations and minimum of machining required

Forward extrusion

Forward extrusion, a basic cold forging operation, reduces slug diameter while increasing length. Stepped shafts and cylinders are typical examples of this process

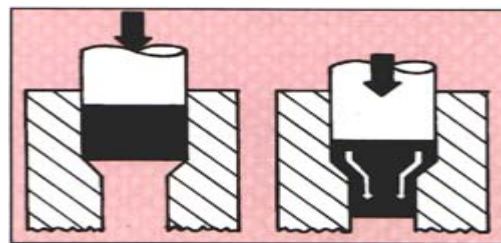


Fig. 1.5 Forward extrusion

Backward extrusion

Backward extrusion, another cold forging process, produces hollow parts. Here, the metal flows back around the descending ram in the opposite direction

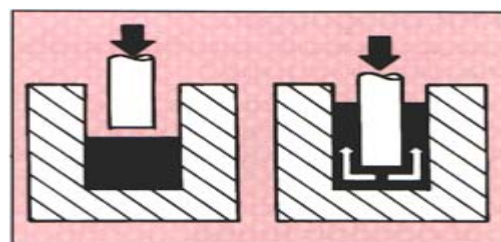


Fig. 1.6 backward extrusion

Lateral extrusion or radial extrusion

It is a special upset forging, where the direction of flow is perpendicular to the punch movement.



Fig. 1.7 Lateral extrusion or radial extrusion

Combination of backward and forward extrusion

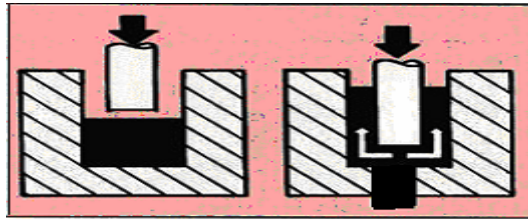


Fig. 1.8 Combination of backward and forward extrusion

Metal forming analysis

The analysis of the stresses in the metal working process has been an important area of plasticity for the past few years. Since the forces and the deformations generally are quite complex. It is usually useful to use simplifying assumptions to obtain a traceable solution. As the strain involved in plastic deformation process is very large, it is usually possible to neglect elastic strain and consider only the plastic strain (rigid-plastic region). The strain hardening is also neglected. The principal use of analytical study of metalworking process is for determining the forces required to produce a given deformation for a certain geometry prescribed by the process and is the ability to make an accurate prediction of the stress, strain, and velocity at every point in the deformed region of the work piece. Since the calculation are useful for selecting or designing the equipment to do a particular job. In this area an existing theory is generally adequate for the task. In general, any theory consists of three sets of equations.

- Static equilibrium of force equation
- Levy Mises equation expressing a relation between stress and strain rate
- Yield criterion

In general case, these are nine independent equations containing nine unknown's six stress components and three strain rate components. While an analytical method is only possible if a sufficient number of boundary conditions are specified, the mathematical difficulties in general solutions are formidable. The most analysis of actual metal working process is limited to two dimensional, symmetrical problems.

The methods of analysis in increasing order of complexity and ability to predict final details are

- The slab method of analysis
- Slip line field theory
- Upper bound solution
- Lower bound solution
- Finite element analysis

The slab method of analysis

This method assumes that the metal deforms uniformly in the deformation zone. A square grid placed in the deformation zone would be distorted into rectangular elements. It is the easiest method and widely used in strength of material. It calculates the inhomogeneity due to friction but neglects the inhomogeneity due to friction at the die-work piece interface and also the influence of transverse stress. It calculates the average forming stress from the work of plastic deformation.

Slip line field theory

This method assumes the nonhomogeneous deformation and is based on the fact that any general state of stress in plain strain consists of pure shear plus a hydrostatic pressure. Slip line is in fact a two dimensional vector diagram, which shows the deviation of maximum shear stress identified with the direction of slip at any point. Slip line is always a network of lines possessing crossing each other at right angle. It is built up by trial and error method.

Lower bound solution

The power of deformation calculated from statistically admissible field which satisfies the

- Stress equilibrium
- Yield criterion

is always lower than the actual one, it is called lower bound solutions. Lower bound solutions are those, which provide values for the total power, which are lower than the actual one. Here the first step is the formulation of a stress tensor, which is far more difficult to conceive. It is

more complex to analyze, so less work has been performed. For lower bound, the requirements are more relaxed and the following conditions are not necessarily fulfilled.

- No need to maintain compatibility
- No need to satisfy stress strain relation
- Geometrical boundary condition don't have to be satisfied

Thus, only equation of equilibrium, yield criterion and statistical boundary condition are the only requirements. The assumed stress field i.e. velocity field is never of such general form as to include all admissible fields due to our limited capability in handling the mathematics in the most general form.

Upper bound solution

An upper bound analysis provides an overestimation of the required deformation force. It is more accurate because it will always result in an overestimation of the load that the press or the machine will be called upon to deliver. In this case factor of safety will be automatically built in. In this analysis, the deformation is assumed to take place by rigid body movement of triangular blocks in which all particles in a given element move with the same velocity.

A kinematically admissible velocity should satisfy the

- Continuity equation
- Velocity boundary condition
- Volume constancy condition

The power of deformation calculated from this is higher than the actual one, called upper bound. When applying upper bound, the first step is to conceive of a velocity field for the deforming body.

- The field can be easily imagined and related to our visual experience.
- Velocity can be measured directly and is easily displayed in a physical manner.
- In this case factor of safety is automatically in built
- It is comparatively easy to analyze.

There exists an infinite no stress field that satisfy the prescribed condition for a lower bound solution and an infinite number of velocity that satisfy the upper bound condition. It is generally assumed that velocity field that the highest lower bound that provides the highest lower bound is closest in characteristics to the actual velocity. Likewise, generally assume a stress field that provides highest lower bound the closest to the actual stress distribution.

Finite element analysis

The finite element analysis method represents an extension of matrix method for the analysis of framed structures to the analysis of the continuum structure. The basic philosophy of this method is to replace the structure i.e. the continuum having an infinite or unlimited number of unknowns by a mathematical model, which has a limited or finite number of unknowns at certain chosen discrete points. This method is extremely powerful as it helps to accurately analyze structures with complex geometrical properties and loading condition.

In finite element method, a structure or a continuum is discretized and idealized by using a mathematical model, which is an assembly or subdivision of discrete elements. These elements known as finite elements are assumed to be interconnected only at the joints called nodes. Simple functions such as polynomials are chosen in terms of unknown displacements and or their derivative at the nodes to approximate over the variation of the actual displacements over each finite element. The external loading is also transformed into equivalent forces applied at the nodes. Next, the behavior of each element independently and later as an assembly of these elements is obtained by relating their response to that of the nodes in a such way that the following basic conditions are satisfied at each node.

- The equation of equilibrium.
- The compatibility of displacements.
- The material constitutive relationship.

The equation, which are obtained using above condition and then these modified equations are solved to obtain displacements at the nodes, which are the basic unknowns of the finite element method.

Finite element method involves extensive computations mostly repetitive in nature. Hence, this method is suitable for computer programming and solutions. Of these problems can be obtained easily using programming on electronic digital computers.

Finite element computer programs have become widely available, easier to use and can display results with attractive graphics. Even an inept user can produce some kind of answer. It is hard to disbelieve finite element results because of the effort needed to get them and the polish of this presentation. However, smooth and colorful stress contours can be produced by any model, good or bad. It is possible that most finite element analyses are so flawed that they cannot be trusted. Even a poor mesh, improper element type, incorrect loads or improper supports may produce results that appear reasonable in casual inspection.

A responsible user must understand the physical nature of the problem and the behavior of finite element well enough to prepare a suitable model and evaluate the quality of results.

Present problem and it's significance

Present problem

In this present work a mathematical by using upper bound method to investigate the load requirements and effect of process parameters of a machine element having radially segmented protrusions around a cylindrical shaft as in spline, spur gear, tracoidal, hexagon & square forms. An optimized velocity field is proposed to obtain better deformation the characteristic for given geometry. From the proposed formulation, effect of no. of protrusions, stroke & friction al conditions are discus in relation to relative punch pressure.

The protrusion of elements having projections, using simple velocity field, the estimated load using their theoretical analysis is approximately 20% higher than their experimental load values.

Significance

Lateral extrusion is a particular form of extrusion and a special branch of closed die forging, is net or near net shape forming process in which a billet is pushed by a punch from a container into the die cavity to deform radially. It is an alter native manufacturing process to

heading and allowing great length to be formed in a single operation. Radial metal flow can be through one or more gaps in the container. Circumferentially a gap in the container allows to production of spur gear, splines, tracoidal, hexagonal & square forms as a consequence of lateral metal flow through these cavities.

Spur gear, splines & hexagon head forms are machine element and mostly used to transmit the load & torque by rotating generally at high speeds. Therefore there is an industrial demand to produce these parts with high strength with in narrow tolerances. It is known that practically deformed gears have a longer life & higher fatigue strength when compared to machined gear formed from same material.

Chapter 2

LITERATURE REVIEW

LITERATURE SURVEY

Parallel to development of three dimensional finite element analyses, a few works on upper bound elemental technique (UBET) have been progressed. Compared with finite element method, the main benefits in applying UBET are the much shorter calculation time and ability to treat the discontinuous material flow that may occur in upset forging.

Because of the industrial significance of upset forging, it has attracted the attention of a number of workers.

JAIN [1] considered the influence of frictional conditions and the material flow during deformation.

MONGAHAN and **BRAYDEN [2]** divided the extrusion forging process into the three stages and has applied the upper bound elemental technique for designing of closed die forging.

V.NAGPAL [3] gave an approach for deriving general kinametically admissible velocity fields for an incompressible material from assumed shape of streamlines. The approach was originally used by **CHEN AND LING [4]** to obtain particular velocity fields for extrusion through some curved dies.

STEPANSKII [5] presented a different upper bound approach for plain strain extrusion wedge shape dies. He assumed a continues radial velocity field for the plastic zone by minimizing upper bound on power, he obtain shapes of curved boundaries separating plastic zone from rigid zones.

AVITZURE [6] presented an exponential function and it also accounts for the buldging of the cylindrical surface during deformation. The velocity field assumed in this analysis however did not satisfy the physical boundary condition and continuity condition.

J.Y.LIU [7] new velocity field for forging of some cylindrical work pieces was presented taking into account the bulging of the free cylinder surface during deformation. The velocity field is more realistic than that proposed by Avitzure [6].

Followings are the some admissible field proposed by various investigators:

[1] Velocity field by **LIU [7]**: Liu presented his velocity field, which is a sine function, and accounts for the bulging of the free cylinder surface during deformation.

As proposed by Liu, Let $g(y)$ be of the form, $g(y) = \sin\left(\frac{b\pi y}{h}\right)$, such that at $y=0; g(y)=0$. The

velocity field becomes,
$$u_r = \frac{b \cdot \pi \cdot u \cdot r \cdot \cos\left(\frac{b\pi y}{h}\right)}{\sin\left(\frac{b\pi}{2}\right)}$$

$$u_y = -1 \cdot \frac{u \cdot \sin\left(\frac{b\pi y}{h}\right)}{2 \cdot \sin\left(\frac{b\pi}{2}\right)}$$

[2] Velocity field by **AVITZURE [6]**: Avitzure presented an exponential function and it also accounts for the bulging of the cylindrical surface during deformation.

As proposed by Avitzure. Let $g(y)$ be of the form, $g(y) = 1 - e^{\left(\frac{-b}{y}\right)}$, such that at $y=0; g(y)=0$. The

velocity field becomes,
$$u_r = \frac{-b \cdot u \cdot r \cdot \cos\left(\frac{b\pi y}{h}\right)}{4 \cdot h} \cdot e^{\frac{-b}{y}}$$

$$u_y = -1 \cdot \frac{u}{2} \cdot \frac{1 - e^{\frac{-b}{y}}}{e^{\frac{-b}{y}}}$$

$$u_\theta = 0$$

Where, the parameter b is responsible for bulging

[3] Velocity field by TRANOVSKI [8]: Tranovski presented his velocity field consisting of two sine functions. Hence two parameters influence the bulging of the cylinder during deformation.

As proposed by Tranovski. Let $g(y)$ be of the form,

$g(y) = b \cdot \sin(\frac{\pi \cdot y}{h}) + b \cdot 2 \cdot \sin(\frac{3 \cdot \pi \cdot y}{h})$, such that at $y=0$; $g(y) = 0$. The velocity field becomes,

$$u_r = \frac{u \cdot r}{4[b_1 - b_2]} \left[\frac{b_1 \cdot \pi}{h} \cdot \sin(\frac{\pi \cdot y}{h}) + \frac{3 \cdot b \cdot 2 \cdot \pi}{h} \cdot \sin(\frac{3 \cdot \pi \cdot y}{h}) \right]$$

$$u_y = \frac{(-1) \cdot u}{2 \cdot [b_1 - b_2]} \left[b_1 \cdot \sin(\frac{\pi \cdot y}{h}) + b_2 \cdot \sin(\frac{3 \cdot \pi \cdot y}{h}) \right]$$

$u_\theta = 0$, b_1, b_2 are the constants.

[4] Velocity field by YANG & KIM [9]: YANG & KIM presented a polynomial function. They also considered the bulging of the cylindrical surface during deformation. They also considered the bulging of the cylindrical surface during deformation. As proposed by Yang & Kim, the velocity field is of the form,

$$g(y) = \frac{-4}{3 \cdot h^2} \cdot y^2 + \frac{2}{h} \cdot y^2 + c \cdot y,$$

Now, at $y=0$; $g(y)=0$. which satisfies the admissibility condition. The velocity field becomes

$$u_r = \frac{u}{2 \cdot h} \cdot r \cdot A \cdot \left[\frac{-4}{h^2} \cdot y^2 + \frac{4}{h} \cdot y + c \right]$$

$$u_y = \frac{-u}{4 \cdot h} \cdot y \cdot A \cdot \left[\frac{-4}{3 \cdot h^2} \cdot y^2 + \frac{2}{h} \cdot y + c \right]$$

$u_\theta = 0$, **A is the constant**

Chapter 3

THEORETICAL ANALYSIS

Upper Bound Elemental Technique

The basic concept of upper bound elemental technique is to break up the work piece into a number of regions. Generally, a kinematically admissible velocity field is constructed for each element. The total consumption of energy is calculated by summing up the consumption values of all the elements. The objective of formulating the UBET is to minimize the total energy rate, of all the elements constituting the entire work piece. The upper bound on the total energy rate is computed by considering.

- The internal homogeneous deformation throughout the deforming zone.
- The energy dissipated due to discontinuous across the internal shear surfaces
- The frictional loss over the tool material interface

The optimal solution is obtained by minimizing the total energy rate with respect to unknown parameters in the velocity field inside the deforming region. In recent decades, several methods to analyze plastic deformation have been developed and applied. Among these are the upper bound element technique (UBET) and finite element analysis (FEA). The upper bound theorem was formulated by Prager and Hodge [10,11]. This theorem states that among a set of given admissible velocity fields for a plastically deforming solid, the best approximation to the actual velocity field is the one that results in the lowest energy dissipation rate. Drucker et al. modified the theorem to include velocity field discontinuities. Kudo [12] introduced the concept of dividing the body into unit deformation rectangular and triangular blocks and studied a variety of unsteady and steady cases of plane strain and axisymmetric deformation. McDermott and Bramley [6] developed additional deformation blocks (which came to be referred to as elements) along with velocity fields and encoded their formulations. This method is known as the UBET. In it, the elemental velocity fields, which minimize mechanical energy dissipation, are determined. Velocity fields are continuous within each element. Normal velocity is continuous at element interfaces. Subsequently, Bramley and coworkers enhanced the UBET to include die fill, elemental

strain accumulation [13], strain-rate hardening [14], and reverse simulation [15]. The UBET has been applied to a variety of metalworking problems [16, 17].

Assumption

- The velocity is uniformly distributed on the UBET element boundary surfaces
- The velocities are linearly varied within each UBET element along the coordinate directions
- The elastic deformation is small compared to the plastic deformation and therefore neglected
- The material is isotropic, homogeneous, rigid plastic and obeys the Von Mises yield criterion
- The material is incompressible, satisfying the relation.
- The frictional shear stress is expressed by a constant friction factor m .
- The tools are absolutely rigid.
- The deformation in the z direction is same for all elements.
- Velocity field is continuous within each element.

Application to the Present Problem

The UBET begins with promulgation of kinematically admissible element velocity fields. These fields apply to specific element shapes (e.g., triangular or rectangular). These fields meet the incompressibility condition and are amenable to the imposition of boundary conditions such as constraint by solid walls or flows from adjacent elements. When an element is adjacent to another element, normal velocity at the interface is made continuous. Analysis are made for all square, hexagonal, trapezoidal and spline section head lateral extrusion processes. As an illustration application of the UBET to spline section head is explained (Fig. 1). The following observations are for this section.

- No metal can cross shear along a plane of symmetry
- The center of cylindrical coordinate r, θ, z is taken at the center of the bottom surface.
- The deformation zone is divided into four regions.
- It is assumed that the velocity discontinuity surfaces between region 1 and 2, region 1 and 3 are of conical surfaces.

- λ is a multiplying factor (one of the optimizing parameter) with height of head which separate the rigid region with deforming zone.

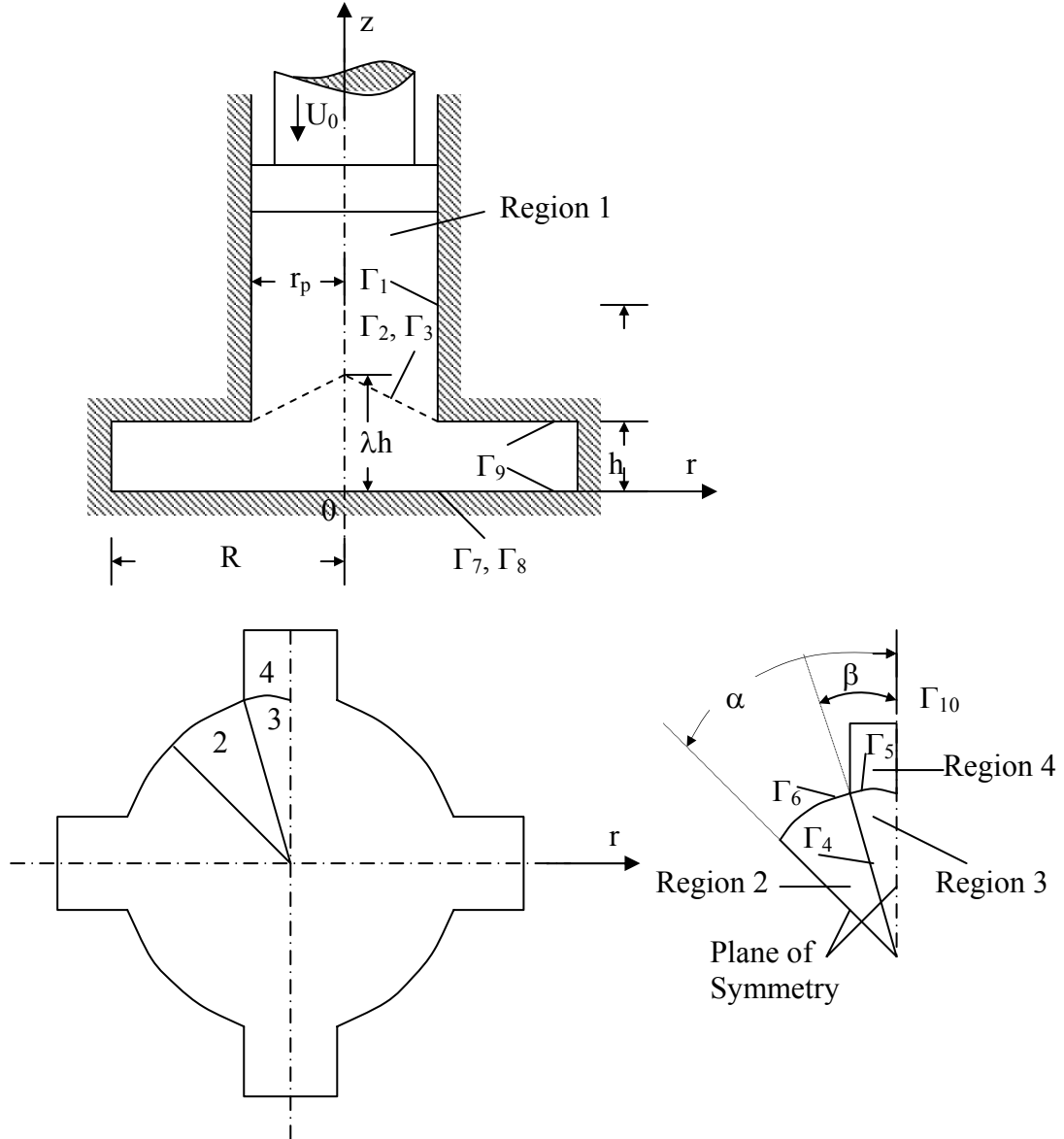


Figure 3.1 Lateral Extrusion for spline with four teeth

As shown in Figure 1, the cylindrical coordinate are taken in such a way that the origin lies at the center of the bottom surface. As punch proceeds, the metal flow into the cavity to deform radially. A radially extruded parts having N protrusions around the cylindrical billet can be divided into $2N$ similar segment (For an illustration a head of 4 spline is taken). Each segment is divided into four segments.

The proposed kinematically admissible velocity field for different regions are:

Region 1: Rigid moving downward with constant velocity, U_0

$$U_r=0, \quad U_\theta=0, \quad U_z=-U_0$$

Region 2: No radial flow, $U_z=0$ at $z=0$, $U_\theta=0$, at $\theta=\alpha$ (plane of symmetry)

$$U_r=0$$

$$U_z = \frac{U_0 z}{2h} \frac{[r_0 + (1 + \lambda)]}{[r_p + (1 - r) + (1 - b)]}$$

Applying continuity condition $\frac{U_r}{r} + \frac{\partial U_r}{\partial r} + \frac{1}{r} \frac{\partial U_\theta}{\partial \theta} + \frac{\partial U_z}{\partial z} = 0$, and boundary condition, we have

$$U_\theta = -\frac{U_0}{2h} r(\theta - \alpha) \frac{[r_0 + (1 + \lambda)]}{[r_p + (1 - r) + (1 - b)]}$$

Region 3: $U_z=0$ at $z=0$, $U_\theta=0$, at $\theta=0$ (plane of symmetry), $U_r=0$ at $r=0$

We assume,

$$U_r = \frac{U_0}{2h} r \frac{\alpha}{\beta} \frac{[r_0 + (1 - d)]}{[r_p + (\lambda - 1)^2]}$$

$$U_\theta = \frac{U_0}{2h} r \theta (\alpha - \beta) \frac{\alpha}{\beta} \frac{[r_0 + (1 - e)]}{[r_p + (\lambda - 1)^2]}$$

Applying continuity condition and boundary condition,

$$U_z = -\frac{U_0 z}{2h} \frac{\alpha}{\beta} \frac{1}{[r_p + (\lambda - 1)^2]} [2\{r_0 + (1 - d)\} + (\alpha - \beta)\{r_0 + (1 - e)\}]$$

Region 4:

$$U_z=0$$

$$U_\theta=0$$

$$U_r = \frac{U_0}{2h} \frac{[(1 - z) + r_0 + (1 - c)]}{r\beta[r_p + (\lambda - 1)^2]}$$

Where,

h = maximum thickness of the head

r_0 = maximum diameter of the head without spline

R = maximum diameter of the head with spline

r_p = diameter of the billet or container

λ = is a multiplying factor (one of the optimizing parameter) with height of head

which separate the rigid region with deforming zone.

b, c, d, e = optimizing parameters

r, θ, z = axis of the cylindrical coordinate system

α = angle made by one symmetrical part (zone of consideration) at center

β = angle made by one half of the spline at center

Applying the upper bound elemental method, the expression for total power consumption, J^* , should be minimised to find the actual velocity distribution, where

$$J^* = \sum \dot{W}_i + \sum \dot{W}_s + \sum \dot{W}_f .$$

W_i is the internal power of deformation, W_s is the power expended at the surfaces of velocity discontinuities between the elements and W_f is the power utilized to overcome frictional resistance at billet-die interfaces.

$$\dot{W}_i = \frac{2}{\sqrt{3}} \sigma_0 \int_v \sqrt{\frac{1}{2} (\dot{\epsilon}_{\theta\theta}^2 + \dot{\epsilon}_{rr}^2 + \dot{\epsilon}_{zz}^2 + 2\dot{\epsilon}_{\theta z}^2 + 2\dot{\epsilon}_{\theta r}^2 + 2\dot{\epsilon}_{rz}^2)} dV$$

$$\dot{W}_s = \frac{\sigma_0}{\sqrt{3}} \int_{\Gamma_s} |\Delta U| dS$$

$$\dot{W}_f = m \frac{\sigma_0}{\sqrt{3}} \int_{\Gamma_f} |\Delta U| dS$$

For cylindrical coordinate, strain rates for all zones can be derived by the following equations:

$$\dot{\epsilon}_{rr} = \frac{\partial U_r}{\partial r}, \quad \dot{\epsilon}_{\theta\theta} = \frac{1}{r} \left(\frac{\partial U_\theta}{\partial \theta} + U_r \right), \quad \dot{\epsilon}_{zz} = \frac{\partial U_z}{\partial z}$$

$$\dot{\epsilon}_{r\theta} = \frac{1}{2} \left(\frac{1}{r} \frac{\partial U_r}{\partial \theta} + \frac{\partial U_\theta}{\partial r} - \frac{U_\theta}{r} \right) \quad \dot{\epsilon}_{\theta z} = \frac{1}{2} \left(\frac{\partial U_\theta}{\partial z} + \frac{1}{r} \frac{\partial U_z}{\partial r} \right)$$

$$\dot{\epsilon}_{rz} = \frac{1}{2} \left(\frac{\partial U_r}{\partial z} + \frac{\partial U_z}{\partial r} \right)$$

For an illustration, for element 3:

$$\dot{\epsilon}_{rr} = \frac{U_0}{2h} \frac{\alpha}{\beta} \frac{[r_0 + (1-d)]}{[r_p + (\lambda - 1)^2]}$$

$$\dot{\epsilon}_{\theta\theta} = \frac{U_0}{2h} \left[(\alpha - \beta) \frac{\alpha}{\beta} \frac{\{r_0 + (1-e)\}}{\{r_p + (\lambda - 1)^2\}} + \frac{\alpha}{\beta} \frac{\{r_0 + (1-d)\}}{\{r_p + (\lambda - 1)^2\}} \right]$$

$$U_z = -\frac{U_0}{2h} \frac{\alpha}{\beta} \frac{1}{[r_p + (\lambda - 1)^2]} [2\{r_0 + (1-d)\} + (\alpha - \beta)\{r_0 + (1-e)\}]$$

$$\dot{\epsilon}_{r\theta} = \dot{\epsilon}_{\theta z} = \dot{\epsilon}_{rz} = 0$$

Total power dissipation, J^* , for all of the regions is obtained by summing up all the power components in the four regions. Externally supplied power is $P_{av} \cdot A \cdot U_o$, where, “ P_{av} ” is the average extrusion pressure, “ A ” is the cross sectional area of the billet and U_o is the ram velocity. Equating external energy supplied during upsetting with total upper bound energy, the non-dimensional forging pressure, $\frac{P_{av}}{\sigma_o}$, is equal to $\frac{J^*}{\sigma_o \cdot A \cdot U_o}$. After minimizing the upper bound on power, J^* , with respect to the optimizing parameters, the coordinates of the deformed work piece can be determined.

Computation

The whole computational procedure used to determine the optimum average extrusion pressure, mainly consists of two parts. The first one is the Gauss ten point quadrature to find out the triple integration for volume. It is applied to get upper bound energy for internal deformation. The second one is programming for optimization in which we find out the proper value of the all the constants, λ , b , c , d and e to get the minimum value of the non-dimensional extrusion pressure. The computational work was done for determining the P_m/σ_o , optimum extrusion pressure with different h/r_p . The theoretical results obtained for non-dimensional average extrusion load are compared with the experimental values. The theoretical and experimental shapes are also plotted & examined.

Chapter 4

EXPERIMENTAL INVESTIGATION

Experimental investigation

Commercially available tellurium lead was chosen as the working material for the experiments (lateral extrusion). Different shape of heads (square, hexagonal, tracoidal and spline) with different thickness (approximately, 15.5, 14.7, 13.8, 12.6mm) was produced.

Determination of Material Behaviour

A serious limitation of the tensile test even for cold working is that fracture occurs at a moderate strain; so that it is not possible to use this test for determination of yield stress, after very heavy deformation. The fracture is most easily avoided by adopting some compressive form of test. The average stress state during testing is similar to that in much bulk deformation process, without introducing the problems of necking or material orientation.

Therefore, in compression test, a large amount of deformation can be achieved before fracture. By controlling the barreling of the specimen ends and the anvils with lubricants the strain can be varied under limits

Compression Test

The simplest of these tests is the axial compression of a cylinder between smooth platens. If the platens are well lubricated, this gives essentially the same yield stress at a tensile test with small strains. As the strain is increased, the specimen spreads and thinning of the lubricant occurs, so that the frictional component at the die face increases. The increase in the load required causing yielding. It can be overcome to a large extent by removing the sample after small increments in strain and relubricating each time. The main disadvantage of this tests is conducted at a constant true stress strain rate require special equipment. Compression testing has developed into a highly sophisticated test of workability cold upset forging and is a common quality control test in forging operation.

Compression loads are applied to many engineering structures that vary in dimension from massive suspension bridge piers to the thin sheets of aircraft wings. In addition, metal forming processes involve large deformation. Analysis of metal forming processes require knowledge of stress strain properties. The following assumptions are made in stress strain testing.

- In any test, used to obtain uniform axial compression stress strain properties, the measured quantities are generally load and strain. If a strain gage is used or displacement is measured at the surface of the specimen, the longitudinal and transverse strain is assumed to be uniform along the entire gage length.
- The cross sectional area is constant over the gage length
- The stress is uniaxial and uniform in each cross section along the gage length
- The loading forces must maintain initial alignment through out the entire loading process
- The measured surface strain is assumed to be same as internal strain.

An error in stress or strain occurs, if the assumptions of uniformity do not exist in a test. Buckling, distributions, and elimination of these phenomena in the compression test leads to more accurate stress strain data.

Experimental Procedure

Cylinders with a 20mm × 30 mm ($H/D = 1.5$) are used to obtain the stress-strain curve by a compression test using UTM at room temperature. The compression rate is maintained same as that adapted for the experiments. The specimen has oil grooves on both the ends to entrap lubricant during the compression test. The compression load is recorded by dial gauge at every 0.5 mm of punch travel. After compressing the specimen to about 15 mm it is taken out of the press, re-machined to cylindrical shape with original diameter, and tested in compression till the specimen is reduced to about 10mm. The stress-strain diagram is drawn and the curve is extrapolated beyond a natural strain 0.5. To simulate a rigid plastic material, the wavy portion is approximated by smooth line (Fig. 4.13). The average flow stress of the used material is found to be 0.225 Tons/cm².

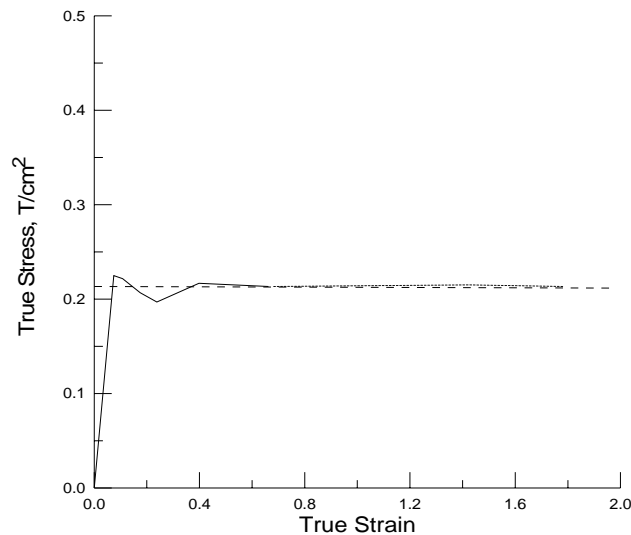


Fig 4.1 stress strain characteristics of Lead in compression test

Measurement of Friction Factor

The local value of the friction cannot be easily determined. The coefficient of friction may actually vary through a working pass, as the lubrication deteriorates due to thinning of the film and extension of their surface. Experimental studies suggests, however that this is negligible for all well lubricated operations. There is at present no generally accepted method of measuring the value of the coefficient of friction for given surface and lubricant. Various factors can influence the result, chemical condition, lubricant film thickness; temperature, speed, environment and degree of deformation should match as closely as possible the actual conditions of the operation. The friction factor can be measured by the following methods.

- Direct measurement of friction in metal working
- Coefficients obtained from correlation of theory
- Measurements depending upon shape change.

Ring Compression Test

If the coefficient of friction can be deduced from a change in shape, the yield stress will not enter the derivation, provided the material is homogeneous and there is no serious temperature gradients. Such methods are generally suitable for rapidly strain hardening materials. Ring compression test suggested by Kudo and Kungio and developed by Cockcroft utilizes axial compression of a ring between flat platens. When a flat, ring shaped specimen is upset in the axial direction, the resulting shape change depends only on the

amount of compression in the thickness direction and the frictional conditions at the die ring interfaces. If the interfacial friction were zero, the ring would deform in the same manner as a solid disk, with each element flowing outward radially from the center.

In case of small but finite interfacial friction, the outside diameter is smaller than in the zero friction case. If the friction exceeds a critical value, frictional resistance to outward flow becomes so high that some of the ring material flows inward to the center. Measurements of the inside diameters of compressed rings provide a particularly sensitive means of studying interfacial friction, because the inside diameter increases if the friction is low and decreases if the friction is higher. The ring thickness is usually expressed in relation to the inside and outside diameters. Under the condition of maximum friction, the largest usable specimen height is obtained with rings of dimensions in the ratio of 6:3:1 i.e outer diameter:inner diameter:height. For normal lubricated conditions, geometry of 6:3:2 can be used to obtain results of sufficient accuracy for most applications. The ring compression test can be used to measure the flow stress under high strain practical forming conditions. Thus, by measuring the ratio of internal, external diameters after axial compression of a ring of standard dimensions, it is possible to obtain a measure of the friction.

Experimental Procedure

A ring compression test was carried out at commercially available grease lubrication condition. The friction factors were found to be **0.38** for the lubricated condition by comparing our result with the calibration curve of Male and Cockcroft (Fig. 4.2).

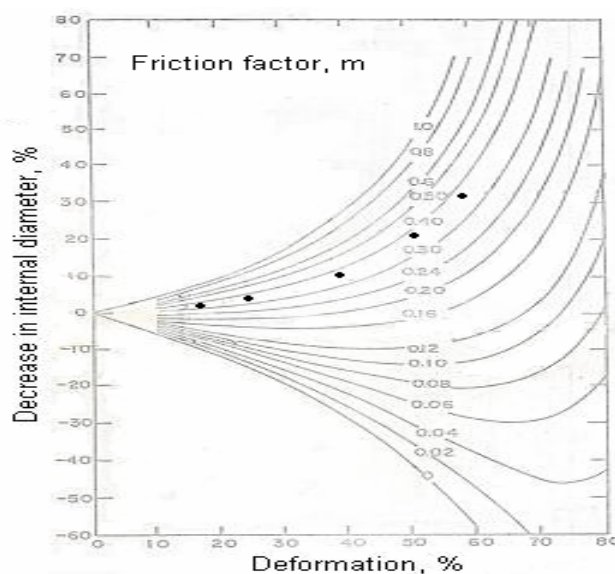


Fig. 4.2 Theoretical calibration curve for standard ring 6:3:2

Experimental Setup

It is a closed die forming & it consist of following basic component, they are namely punch, container, die, die holder & base plate and are assembled by four M16 bolts. The dimensions of all these parts is mention in the Figs 4.3-4.5. These are all made of mild steel & is used for extrusion of lead.

The billet is placed in the container with die, die holder, and base plates are tightened from the bottom. The punch is now inserted from the top of the container and forced the billet down.

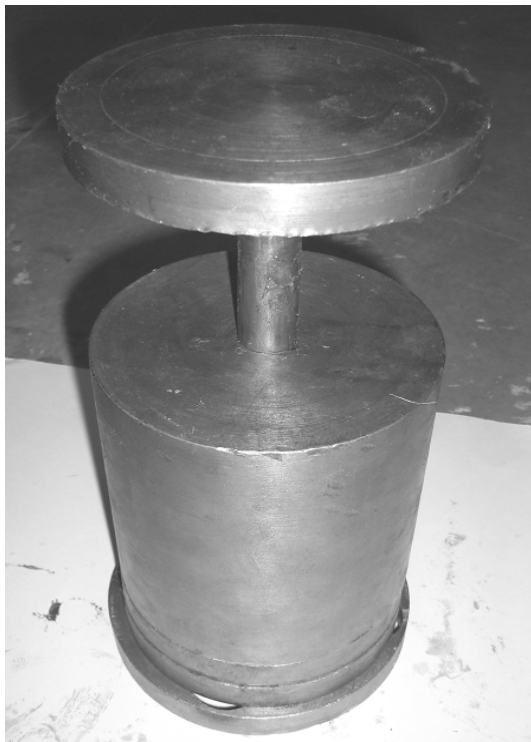


Fig. 4.3 Assembled Setup

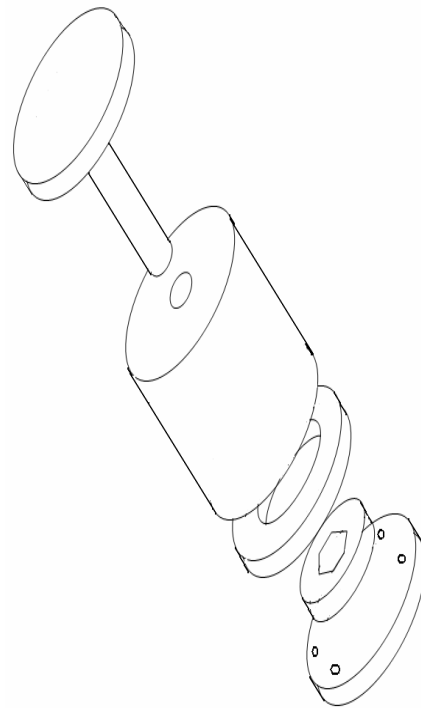


Fig. 4.4 Exploded Drawing of Assembled Setup



Fig. 4.5 Different Parts of the Setup

Materials of Parts

Container with extrusion chamber

Material: MS

Properties: tensile strength – 320 N/mm²

hardness – 100 BHN

Die plate

Material: MS

Properties: tensile strength – 320 N/mm²

hardness- 100 BHN

Punch & supporting plate

Material: MS

Properties: tensile strength – 320 N/mm² hardness- 100 BHN

Bolt

Material: harden steel

Properties: tensile strength – 390 N/mm²

hardness- 200 BHN

Extrude metal

Material: lead

Properties: tensile strength – 20 N/mm²

melting point –327 C

density –11330 Kg/m³

Rough Design of Experimental Setup

Extrusion pressure

Considering the maximum area reduction (i.e. 90 % for design safety) from existing theoretical analysis, average extrusion pressure P_{av} can be found out using

$$P_{av} = \sigma_0 (1.06 + 1.55 \ln 1/(1-R)) \text{ N/mm}^2$$

Where, σ_0 = yield strength in uniaxial compression of lead

R = friction area reduction

(With factor of safety = 3)

Punch or ram

In extruding process the punch / ram may be failed either by crushing or buckling.

Considering the buckling failure:

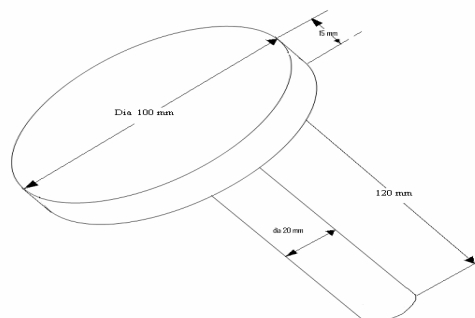


Fig. 4.6 Dimension. of punch or ram

$$P_{av} \times A = 2\pi^2 EI / L^2$$

A=cross sectional area of punch

L=length

E=young modulus

I=moment of inertia

Assuming the adequate safety the length of punch is taken as 120 mm and cross section area 300 mm² the crushing strength of the punch is also more than the maximum extrusion pressure applied.

Die plate

Considering the shear failure, the thickness of die plate t , is such that it obeys

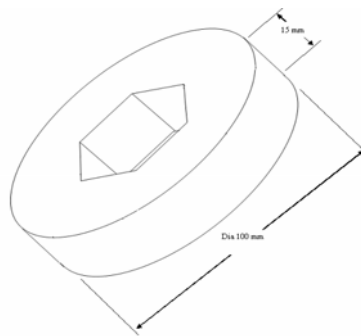


Fig. 4.7 Dimension of die

$$L \times f_s \times t = P_{av} \times A$$

where L = total length

f_s = shear strength of die holder

thickness of die plate is taken as 15 mm. considering design safety.

Die holder

It has a center through hole of 30 mm dia for extruded product to eject out with no obstacles.

The thickness or height H , is taken such that it will not fail by shear

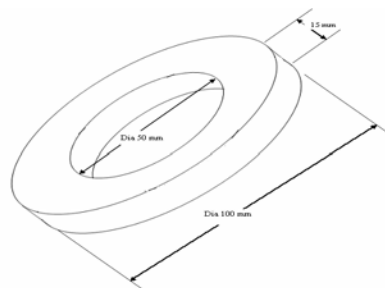


Fig. 4.8 Dimension of die holder

$$L \times f_s \times H = P_{av} \times A$$

where, L= total length

f_s =shear strength of die holder taking $H = 70$ mm and & outer dia of holder 125 mm it will remain well with in design safety

Container with extrusion chamber

The length or height of the container T, is taken as 120 mm and outer dia is 120 mm and checked for crushing or /and shear failure

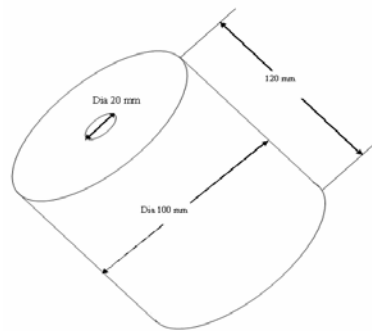


Fig. 4.9 Dimension of container

$$A_c \times f_c = P_{av} \times A$$

$$A_s \times f_s = P_{av} \times A$$

Where, A_c = total crushing area

A_s = total shear area

f_s = shear strength of die

f_c = crushing strength of container

it is found well with in limit

Bolt

The dia & no. of bolt used to secure the container and die holder such that they will not fail by maximum possible extrusion load

$$\frac{\pi}{4} d^2 \times f_s \times 2 = P_{av} \times A/N$$

where d = dia of bolt

N = no. of bolt

f_{s2} = shear strength of bolt

Two bolts of 16 mm dia secure the assembled set up well within safety

Calculation of Effective Length

Different dies have different volume, so we need to calculate what is the specimen length required to fill the die completely. This is nothing but the effective length of the specimen which is required to be deformed and the readings are taken up to that.

SQUARE

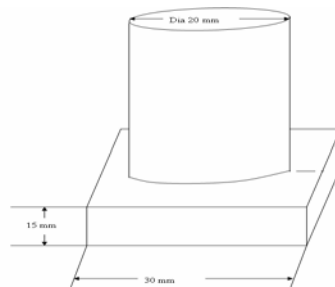


Fig. 4.10 Dimension of square product

Side (l) = 30 mm

Area (A) = $l^2 = 900 \text{ mm}^2$

Volume (V) = $A \times h = 13500 \text{ mm}^3$

Effective length (l_e) = $V/A1 = 42.97 \text{ mm}$

Area of specimen ($A1$) = 314 mm^2

HEXAGON

Side (l) = 17.32 mm

Area (A) = $3/2 \times l \times d = 779.42 \text{ mm}^2$

Volume (V) = $A \times h = 11691.34 \text{ mm}^3$

Effective length (l_e) = 37.21 mm

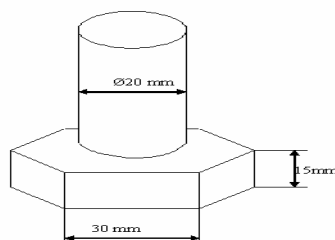


Fig. 4.11 Dimension of hexagon product

SPLINE

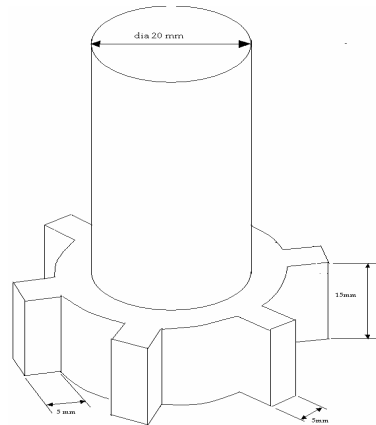


Fig. 4.12 Dimension of spline product

$$\text{Area (A)} = 856.85\text{mm}^2$$

$$\text{Volume (V)} = 12852.87\text{mm}^3$$

$$\text{Effective length (le)} = 40.91 \text{ mm}$$

$$\text{Effective length (le)} = V/A1 = 40.91 \text{ mm}$$

TROCOIDAL

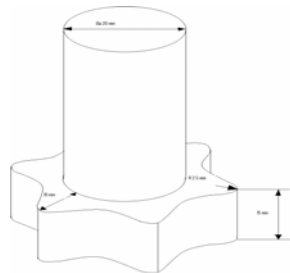


Fig. 4.13 Dimension of trochoidal product

$$\text{Area (A)} = 949.08\text{mm}^2$$

$$\text{Volume (V)} = 14236.27\text{mm}^3$$

$$\text{Effective length (le)} = 45.31 \text{ mm}$$

Lateral Extrusion of Different Shapes

Experiments for lateral extrusion of different polygon head bolts were carried out in a 60 ton Universal testing machine (Figs. 4.14-4.15) at room temperature. Commonly available lead was chosen as the working material with specimen dia of 20 mm & 90 mm length cylindrical specimen. The speed of UTM is maintained uniform approximately at 2mm per minute to minimize rate effect. The billets were compressed up to reduction of about fifty percent in height continuously. Load was measured with stroke and the nature of variation is observed. Different shapes after extrusion are shown in photographs (Figs 4.16 -4.19). Fig. 4.20 shows the photograph of spline headed products applied with different load to find the amount of flow. This experiment is being repeated for no. of times with varying the die height. Placing the thin sheet of aluminum inside the die can vary this height. The experiment is done individually for different dies and readings are recorded. The variation of extrusion pressure with stroke is shown in Figs 4.21-24. This shows that the lateral extrusion process consists of five stages:

- Initial compression stage, in which load increase linearly.
- Initiation of flow of metal stage, in which load remains constant.
- Obstruction of flow stage, in which load increases depending on head shape.
- Smooth flow stage inside obstruction, in which load remains approximately constant.
- Final closing stage, in which load increases steeply as the head cavity filled up.

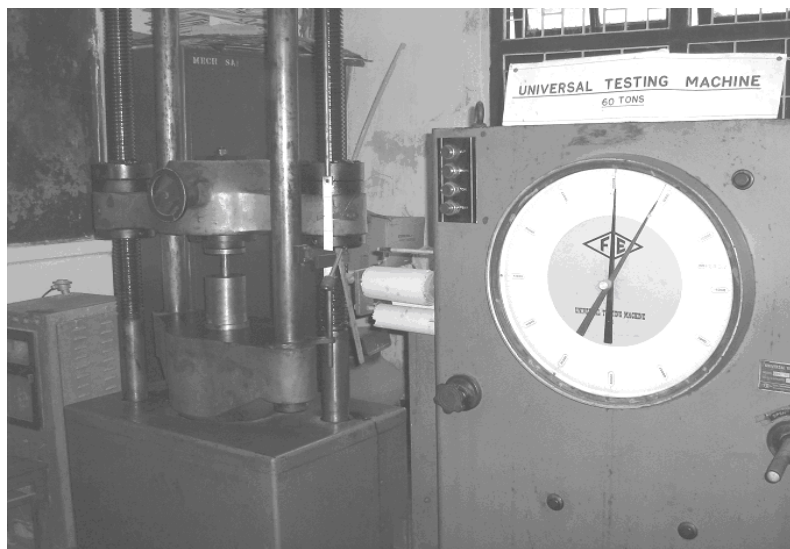


Fig. 4.14 Experimental Setup on UTM

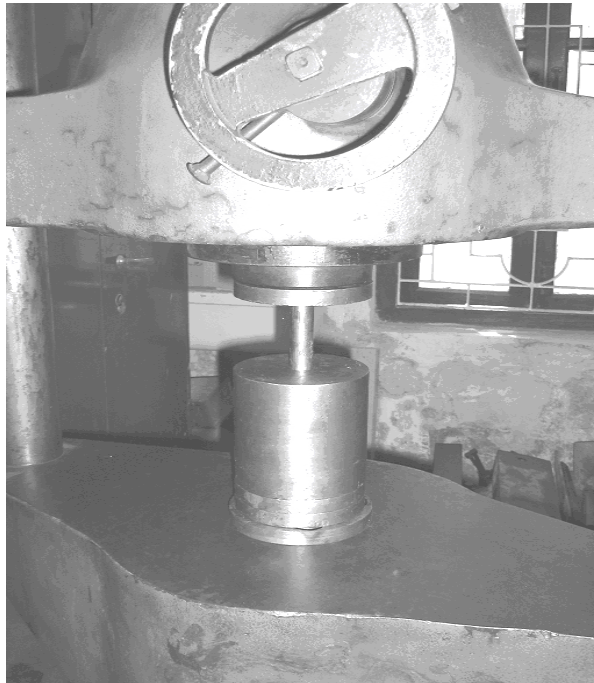


Fig. 4.15 Experimental Setup on UTM (close view)

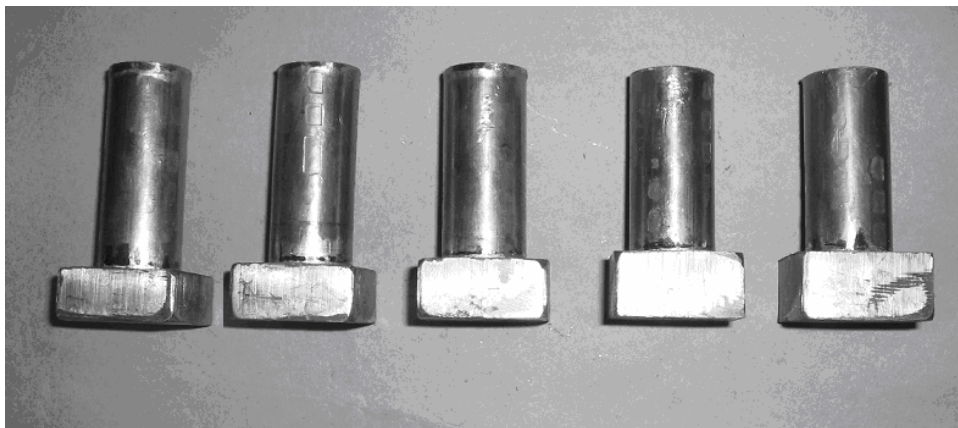


Fig. 4.16 Photographs of Products (Square head)



Fig. 4.17 Photographs of Products (Hexagonal head)

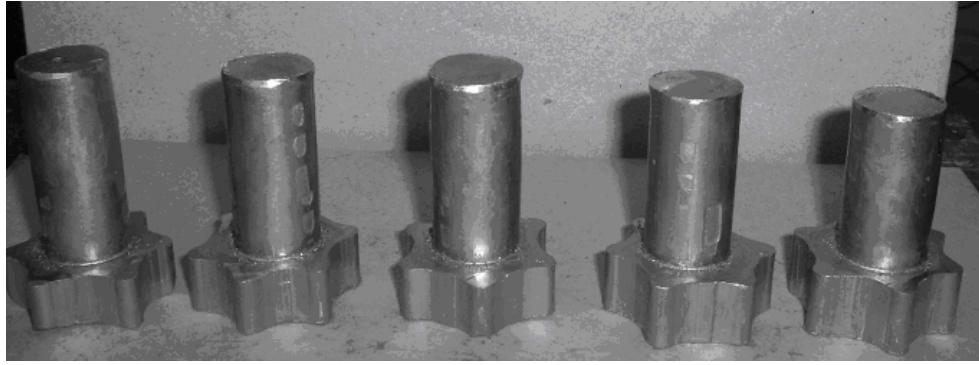


Fig. 4.18 Photographs of Products (Tracoidal head)



Fig. 4.19 Photographs of Products (Spline head)



Fig. 4.20 Photographs of Products (Spline head) with Different Load

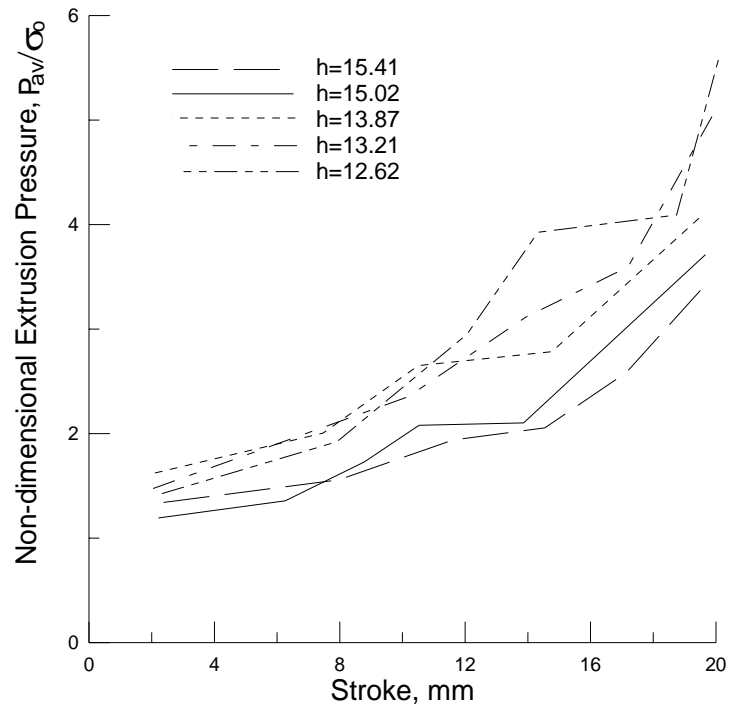


Fig. 4.21 Variation of extrusion pressure with stroke (Square head)

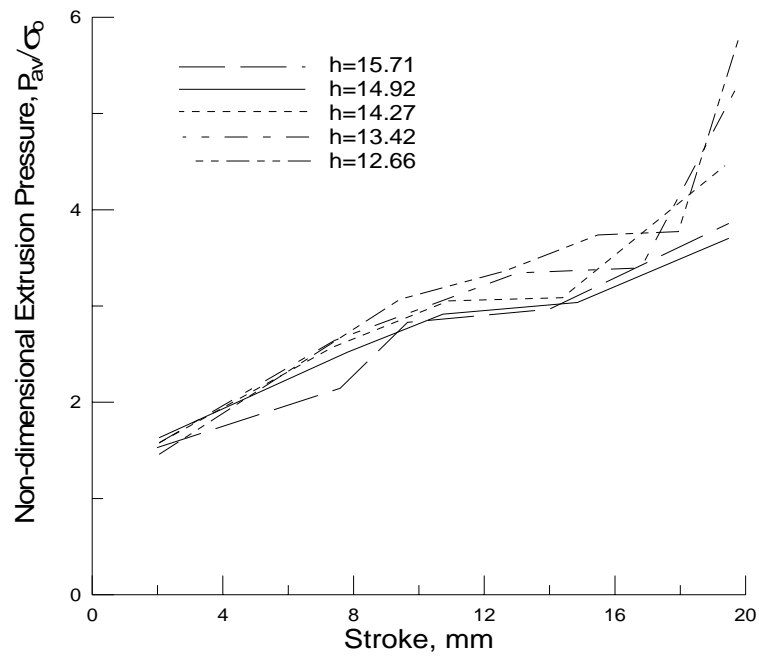


Fig. 4.22 Variation of extrusion pressure with stroke (Hexagonal head)

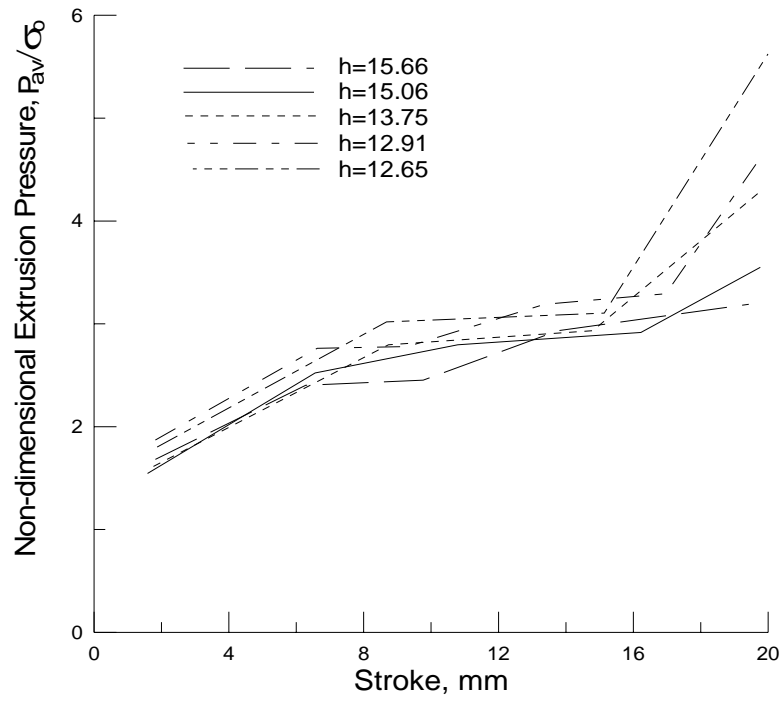


Fig. 4.23 Variation of extrusion pressure with stroke (Tracoidal head)

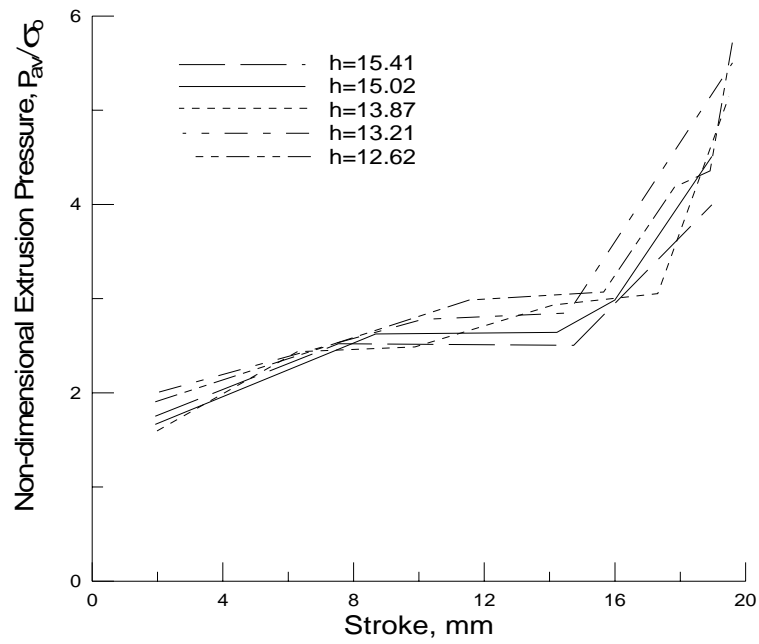


Fig. 4.24 Variation of extrusion pressure with stroke (Spline head)

Chapter 5

**APPLICATION OF THE ALGOR
SOFTWARE**

ALGOR

ALGOR, mission is to pioneer high technology analysis and prediction tools that enable engineers to create safe, efficient, and cost effective designs. Since introducing finite element analysis for PCs in 1984 and interfacing with CAD systems in 1985, ALGOR has emerged as a dynamic player in the computer aided engineering software industry. More than 20000 engineers worldwide have chosen ALGOR software.

ALGOR offers nonparallel engineering technology for every analysis need, including mechanical event simulation for motion and stress analysis, finite element analysis. INCAD technology for CAD/CAE interoperability and piping system design and analysis. Using ALGOR, engineers can analyze stresses and displacements in complex parts due to static or dynamic loading applied constantly or varying with time. Effects of large deflections under these loading can be analyzed using a variety of nonlinear material models. ALGOR can also be used to analyze the effects of thermal loads on parts and will provide results such as a temperature profile or heat flow through a particular area. ALGOR also provides such as temperature profile or heat flow through a particular area. ALGOR also provides fluid flow, electrostatic processors to enable engineers to analyze the effects of a wide range of phenomena.

Features

ALGOR products are based on the finite element method. Some unique factors include:

- Internationalized language support allowing easy selection of the language of choice, including Chinese (simplified), English, French, German, Italian and Spanish
- Cost-effective solutions for networked license sharing; enterprise-wide and remote-use licensing; and single, node-locked licensing
- Direct data exchange and full associatively with most CAD solid modelers through a single user interface available for all analysis types

- Industry-recognized, parametric, feature-based modeling system for creating 3-D solid models of parts and assemblies
- Super draw tools for 2- and 3-D sketching, modeling and structured meshing
- An automatic, hex-dominant hybrid meshing tool to produce higher quality elements on the first pass and more accurate results
- MES for combining large-scale motion and stress analysis in a single process, which simulates real-world conditions more accurately
- Specialized FEM piping and pressure vessel system design and analysis tools to verify compliance with international codes
- Full compatibility with industry-standard NASTRAN input and output files so that NASTRAN and/or FEMAP users can benefit from our value-added capabilities including an easy-to-use single user interface, full CAD/CAE associatively with most CAD solid modelers, automatic brick and tetrahedral solid meshing and complementary analysis tools such as fluid flow and MES for combined motion and stress analysis
- Open design environment for engineering data sharing and expansion of technology partnerships

Partnerships with other leading mechanical engineering software companies offer direct data exchange with products from Alibre, Inc.; ANSYS, Inc.; AutoDesk, Inc.; Kubotek USA, Inc.; MSC. Software Corporation; Parametric Technology Corporation (PTC); Robert McNeel & Associates; Solid Edge from UGS; Solid Works Corporation, a Dassault Systems S.A. company; and others. ALGOR's product development process is customer-driven and responsive to market needs with frequent software updates. To assure high, consistent quality in our software products, ALGOR's product development methodology is designed to comply with 10CFR50 Appendix B and 10CFR21 US nuclear requirements and ISO9001 standards.

Steps in ALGOR Analysis

The larger analysis has been completed in two parts. One is modeling and the second one is the analysis part.

Modeling Part

STEP NO	COMMAND	EXPLANATION
1	Start: program: autoCAD2000	In the window task bar, press the “ start ” button, select the programs pullout menu and select the “autoCAD2000”
2	New	Click on the new icon in the left side of the dialog
3	“SQUARE”	Type file name “square” and click save and save
4	DRAW: RECTANGLE	Click on draw on the top menu and select rectangle from the pull down menu
5	Length & width	Enter dimension of the square and complete the drawing
6	EXTRUDE	Give extrude command in the command dialog box And next specify the extrude height
7	CIRCLE	Type circle command in the command dialog box And specify the diameter of the circle
8	EXTRUDE	Give extrude command in the command dialog box And next specify the extrude height from the top surface of the square
9	Union	Type the union command in the command dialog box. And select both the drawing, make ok
10	FILE: EXPORT	Go to file and drag pull down menu and select export. Make the file type to be “AIST”

Hence one modeling has been completed; similarly this process has to be repeated for the other modeling.

Analysis Part

STEP NO	COMMAND	EXPLANATION
1	Start: Program: ALGOR: V17: FEMPRO	In the window task bar, press the “ <u>start</u> ” button, select the programs pullout menu and select the “ <u>ALGOR</u> ” PULL OUT MENU AND SELECT THE “ <u>FEMPRO</u> ”
2	“ <u>open</u> ”	Click on the open icon in the left side of the dialog
3	Select the AutoCAD file	Select the saved AutoCAD AIST file. Hence the model has been opened in the cad environment.
4	Generate mesh	Select the mesh pull down menu from the top and select automatic meshing
5	FEA environment	Click on the FEA environment at the left down side, hence the model will be transferred to FEA environment
6	Element type: brick	Right click on the tree view & Select the brick element type
7	Element definition: isotropic	Right click on the tree view & Select the isotropic element definition
8	Material selection	Right click on the tree view & Select the lead material
9	Add: surface boundary condition	Select all the surfaces except top and right click on the screen, click on add: surface boundary condition: click on fixed on the dialog box
10	Add: surface force	Select the top surfaces, right click on the screen and click on add: surface force: enter the

- | | | |
|----|-----------------------------------|--|
| | | magnitude and direction of force action |
| 11 | Analysis: check model | Access the “ analysis ” pull out menu from the
Then select the “ check model ” command |
| 12 | Analysis: perform analysis | Access the “ analysis ” pull out menu from the
Then select the “ perform analysis ” command |

Hence the complete analysis will be performed and the result will be displayed on the 3D view in the result environment.

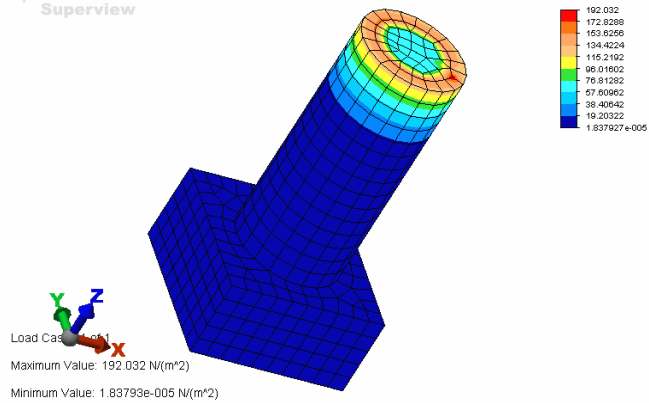
Boundary Condition and Surface Load

In this present problem, as all the surface is fixed, it was assumed that all surfaces are constrained in their respective direction. The top surface can free to move along Z-direction. So the boundary condition for this surface is constrained along X,Y-direction.

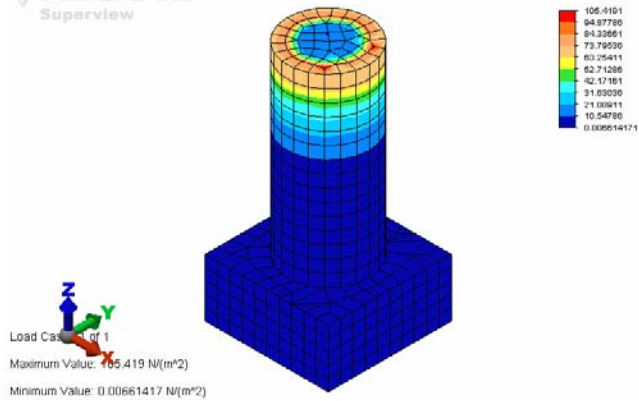
Since our aim is to finding out the stress induced in the different region. So surface displacement boundary conditions are not so important to apply, so it is made to be fixed ie. “add” select the surfaces and make it fixed.

Simulation Results

ALGOR.
Superview

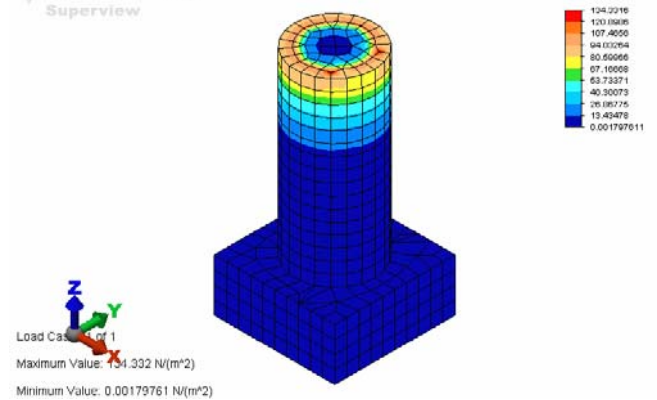


ALGOR.
Superview



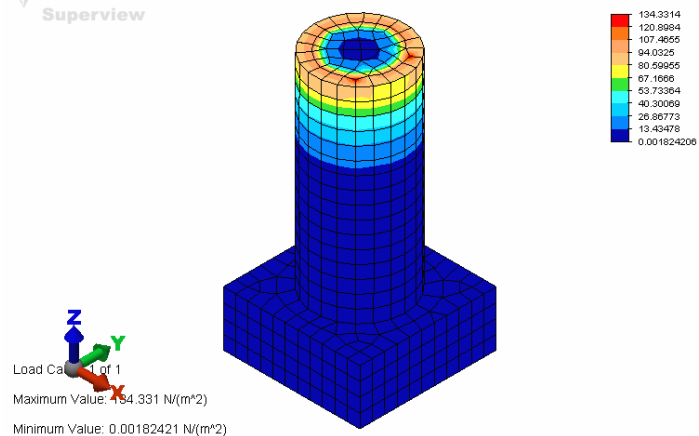
Product with 14 mm head

ALGOR.
Superview



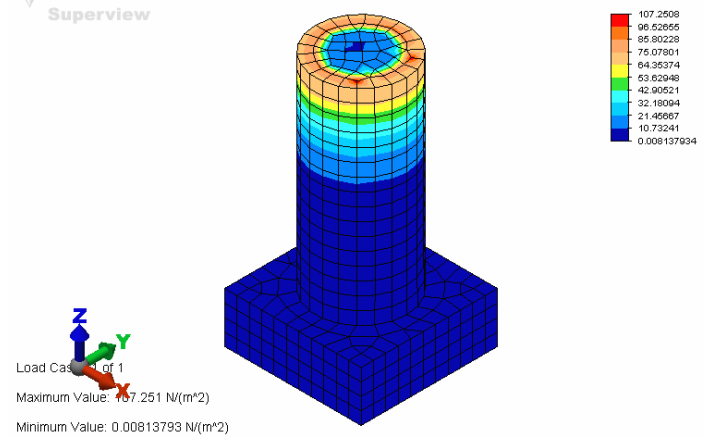
Product with 13 mm head

ALGOR.
Superview

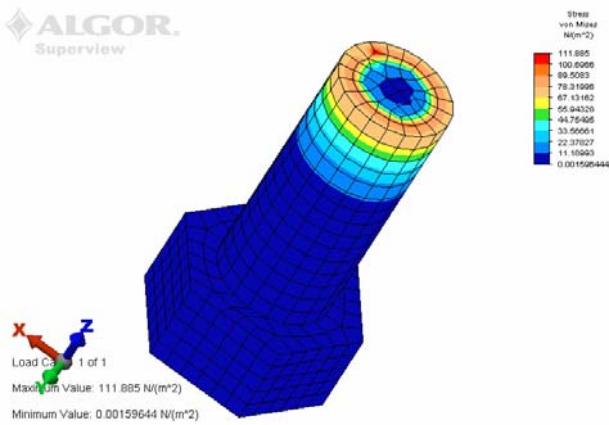


Product with 12 mm head

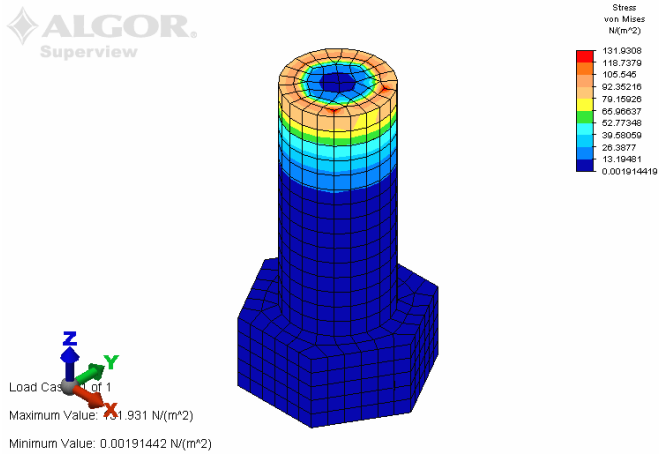
ALGOR.
Superview



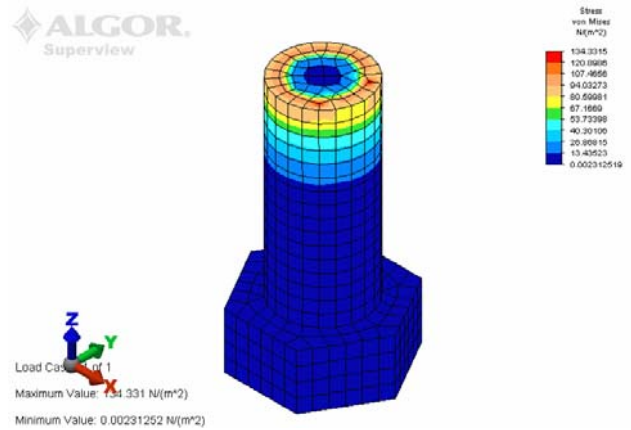
Product with 11 mm head



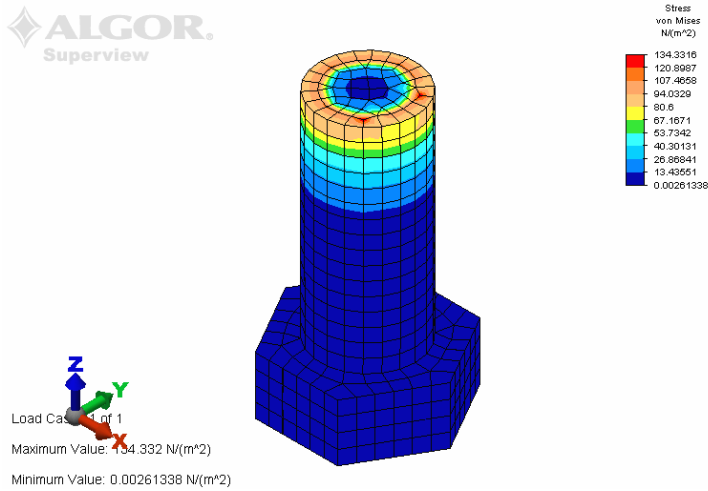
Product with 15 mm head



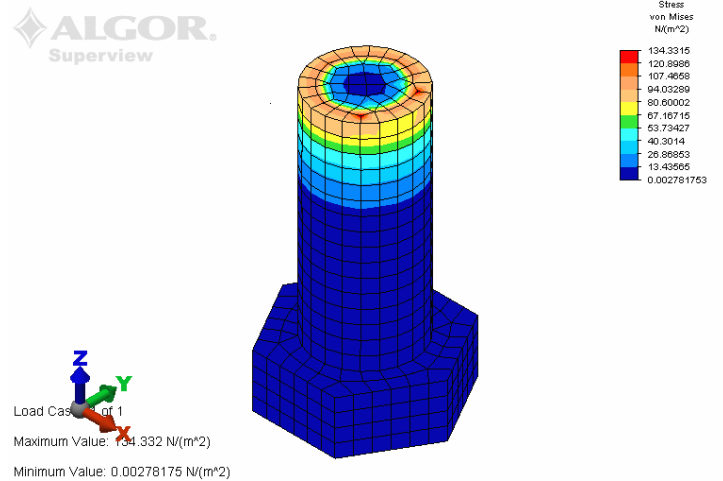
Product with 14 mm head



Product with 13 mm head

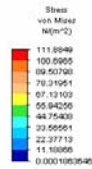
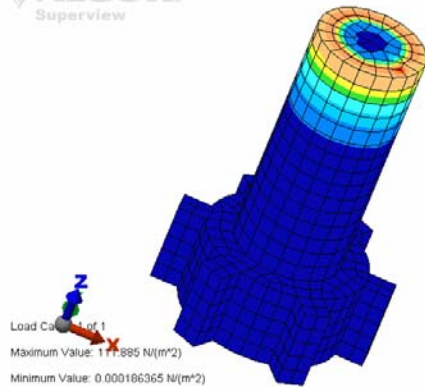


Product with 12 mm head



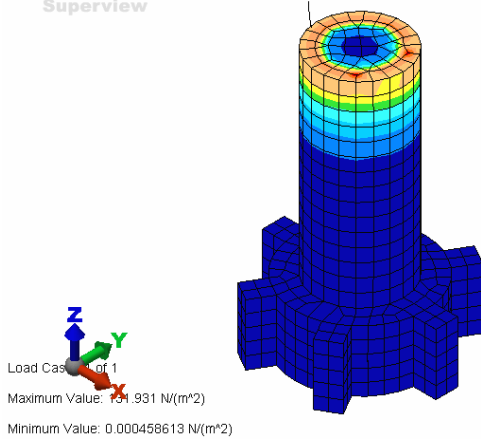
Product with 11 mm head

ALGOR.
Superview

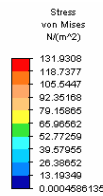


Product with 15 mm head

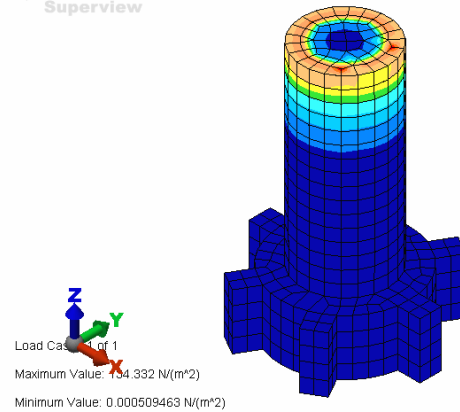
ALGOR.
Superview



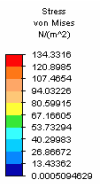
Product with 14 mm head



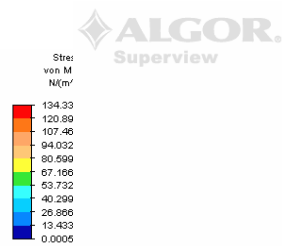
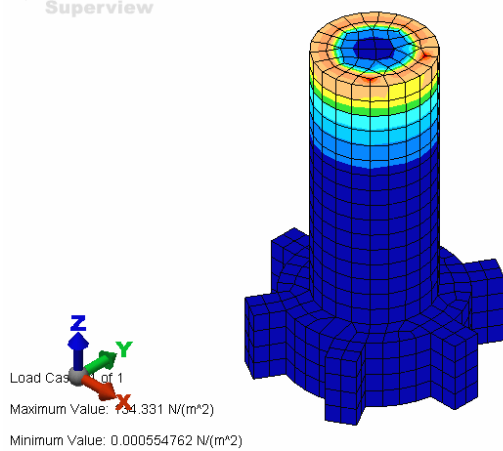
ALGOR.
Superview



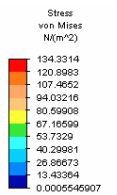
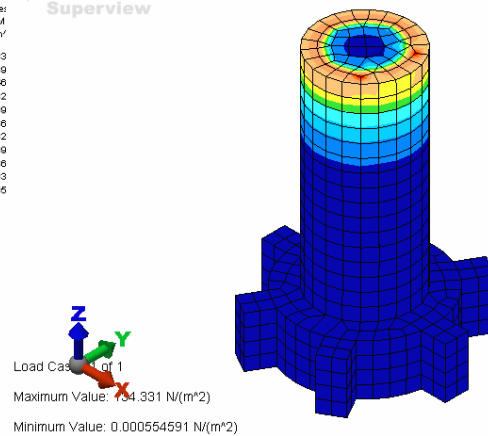
Product with 13 mm head

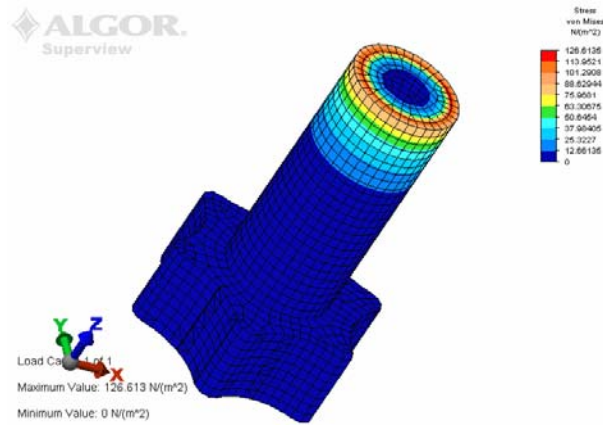


ALGOR.
Superview

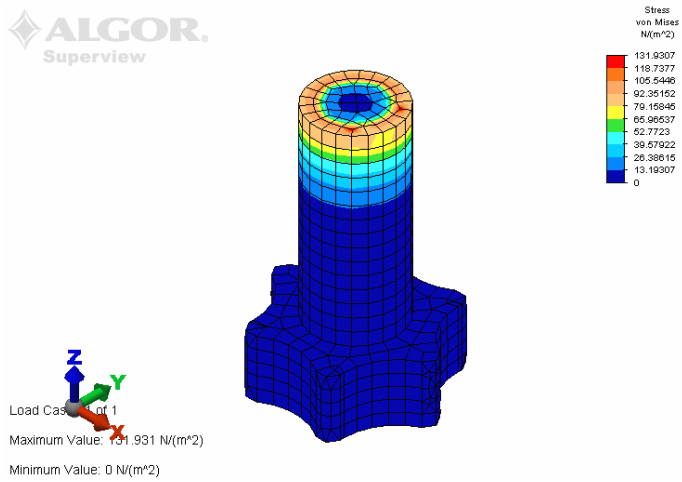


ALGOR.
Superview

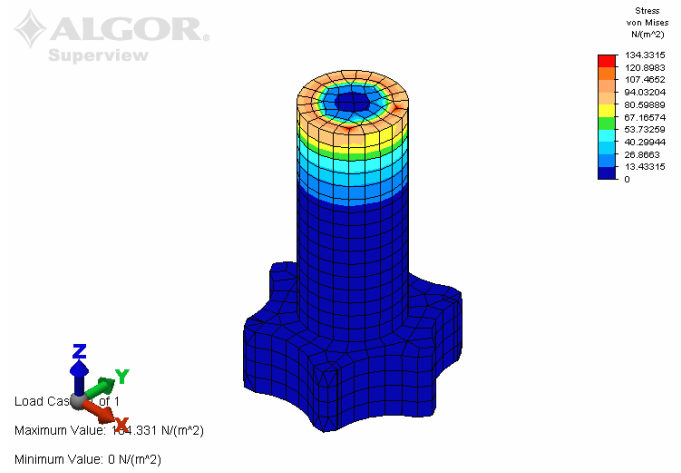




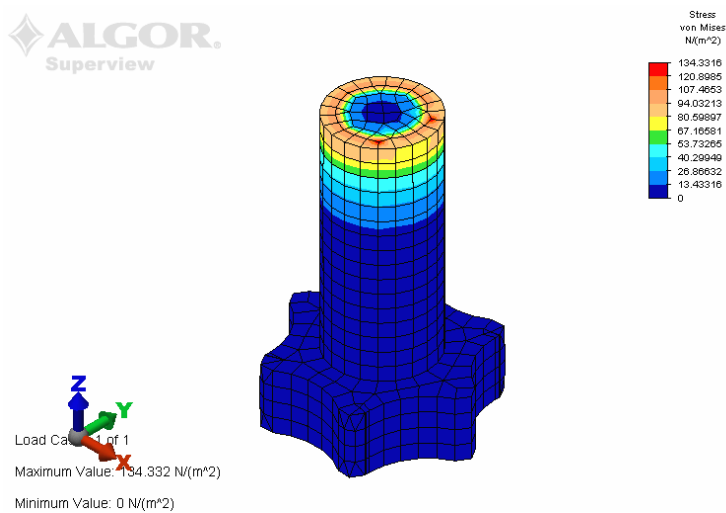
Product with 15 mm head



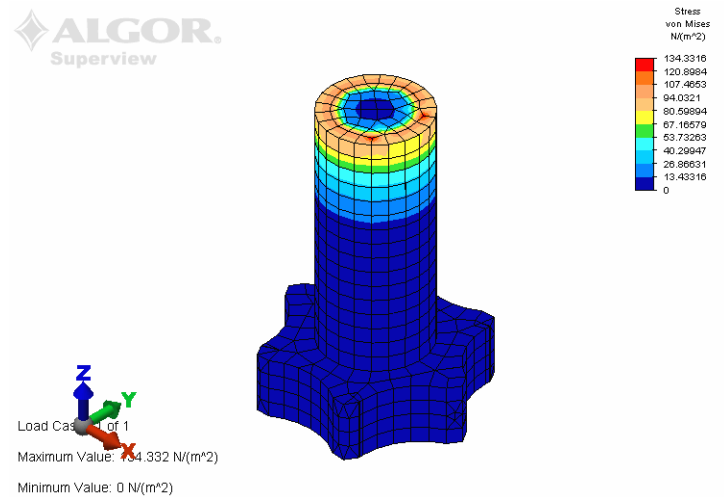
Product with 14 mm head



Product with 13 mm head



Product with 12 mm head



Product with 11 mm head

Discussion and Conclusion

The stress distribution for different head thickness indicates there is an increase in stress at top (close to punch contact) marginally, which is close to both experimental and analytical value. But the stress does not transfer to below (head part), which may be due to incapability of the used commercial package to take care of non-linearity properties of the material, the frictional condition and internal deformation.

Chapter 6

RESULTS & DISCUSSION

Results and discussion

The proposed formulation for the assumed kinematically admissible velocity field is applied to lateral extrusion of bolt with different shape of heads (square, hexagon, tracoidal and spline) with different heights. Experiments are also carried out to validate the proposed analytical model. Numerical calculations have been made for different heights of head.

Each term of the upper bound equation for four regions is solved numerically and a total upper bound equation is optimized with respect to a parameters, λ , b , c , d and e . λ defines the shape of shear surface between the body region and the spline region in region 2 and region 3. The influence of the billet diameter and thickness of the spline on the relative punch pressure are investigated. The effect of ratio of thickness of the spline to billet radius, h/r_p , on the relative punch pressure for given number of teeth (four) and friction condition ($m=0.38$) is shown in Fig. 6.1 for square section, in Fig. 6.2 for hexagonal section, in Fig. 6.3 for tracoidal section and in Fig. 6.4 for spline section respectively with a comparison to the data obtained experimentally. It is seen that as h/r_p increases the relative punch pressure decreases. An increase in head thickness for constant r_p causes a decrease in the h/r_p ratio. Therefore, a thinner head at same friction condition and same number of sides needs a higher forming load because metal flow through a narrow gap is more difficult. On the other hand, the upper bound solution optimized with respect to λ gives a lower value than that when $\lambda = 1$. The discrepancy between optimized upper bound solution and the upper bound solution for $\lambda = 1$ gets bigger as h/r_p decreases.

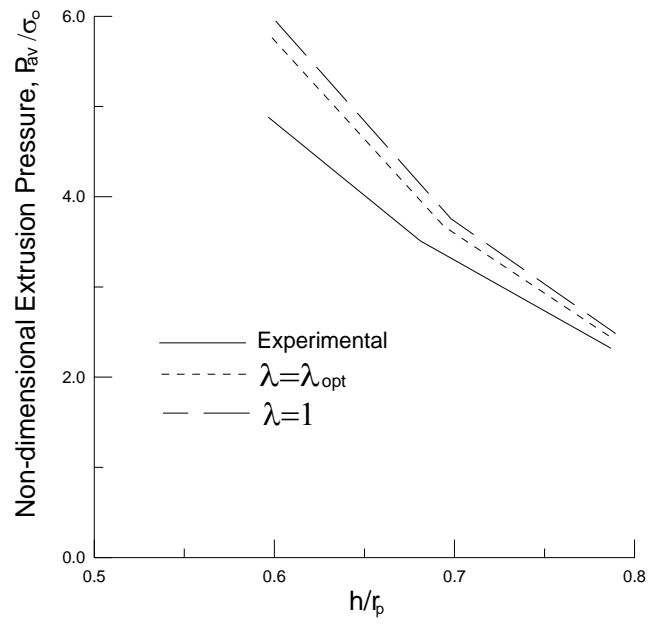


Fig. 6.1 Variation of extrusion pressure with h/r_p (Square head)

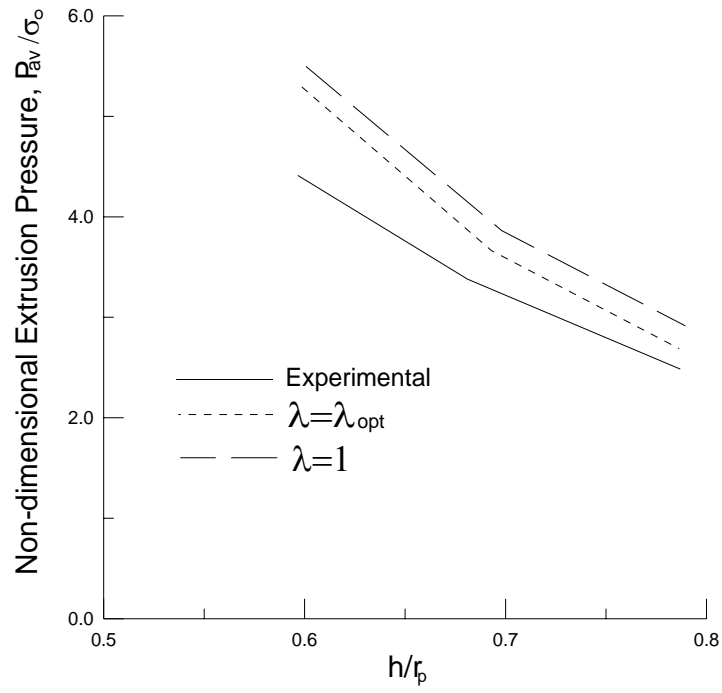


Fig. 6.2 Variation of extrusion pressure with h/r_p (hexagonal head)

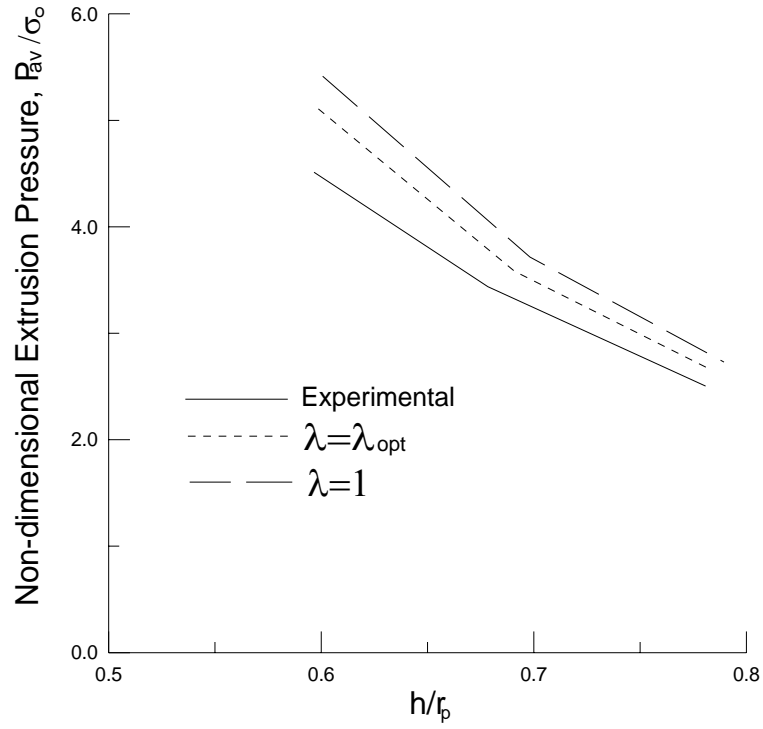


Fig. 6.3 Variation of extrusion pressure with h/r_p (Tracoidal head)

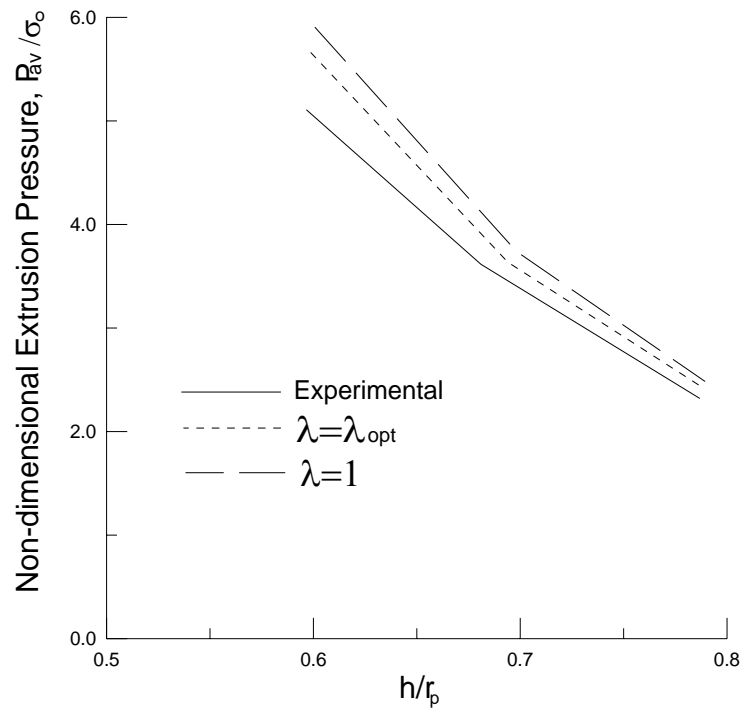


Fig. 6.4 Variation of extrusion pressure with h/r_p (Spline head)

Chapter 7

CONCLUSIONS

&

FUTURE RECOMMENDATIONS

Conclusions and Future recommendations

- Decreasing thickness of the head with a constant billet diameter and friction factor causes a higher relative extrusion pressure.
- The proposed simple kinematically admissible velocity fields to describe the three-dimensional deformation have a qualitative agreement with the experimental results.
- The proposed velocity field gives higher load values than the values experimentally obtained within 25 percent.
- The velocity field proposed in the present investigation can be used conveniently with short computational time for the prediction of extrusion loads & deformations in heading of different shapes.
- A higher order polynomial velocity field can be tested to get better results for different section.

References

References

1. H. Kudo, Some analytical and experimental studies of axisymmetric cold forging and extrusion, *Int. J. Mech. Sci.* 3 (1961) 91-117.
2. S. Kobayashi, Upper bound solutions of axisymmetric forming problems- I, *Trans ASME Series B J. Eng. Ind.* 86 (2) (1964) 122-126.
3. S. Kobayashi, Upper bound solutions of axisymmetric forming problems – II, *Trans ASME Series B J. Eng. Ind.* 86 (2) (1954) 326-332.
4. J.Y. Liu, Upper bound solutions of some axisymmetric cold forging problems, *Trans ASME Series B J. Eng. Ind.* 91 (193) (1954) 1134-1142.
5. L.G. Stepankii, The boundaries of the area of plastic deformation in extrusion, *Russian Eng. J.* 23 (1963) 40-48.
6. V. Nagpal, General kinematically admissible velocity fields for some axisymmetric metal forming problems, *Trans ASME Series B J. Eng. Ind.* 96 (1974) 1197-1201.
7. P.C.T. Chen, F.F. Ling, Upper bound solutions to axisymmetric extrusion problems, *Int. J. Mech. Sci.* 10 (1968) 863-874.
8. Y.D. Yang, H.J. Kim, An analysis of three dimensional upset forging of elliptical disks, *Int. J. MTDR* 26(2) (1986) 147-156.
9. I. Tarnovskii, A.A. Ya Podeyev, V.B. Lyashkov, *Deformation of metals during rolling*, 1st ed., Pergamon Press, New York, USA, 1965.
10. B. Avitzur, *Metal forming process & analysis*, 1st ed., MC Graw - Hill Book Company; New York, USA, 1968.
11. B.L. Juneja, Forging of polygonal disks with barreling, *Int. J. Mach. Tool Des. Res.* 13 (1973) 87-97.
12. B.L. Juneja, Forging of rhombus shaped disks, *Int. J. Mach. Tool Des. Res.* 13 (1973) 99-110.
13. Conor McCormack, John Monaghan, A finite element analysis of cold-forging dies using two- and three-dimensional models, *J. Mater. Process. Technol.* 118(1-3) (2001) 286-292.
14. Guoqun Zhao, Guangchun Wang, V. Ramana Grandhi, Die cavity design of near flashless forging process using FEM-based backward simulation, *J. Mater. Process. Technol.* 121(2-3) (2002) 173-81.
15. Y.K Lee, S.R Lee, C.H Lee, D.Y Yang, Process modification of bevel gear forging

- using three-dimensional finite element analysis, *J. Mater. Process. Technol.* 113(1-3) (2001) 59-63.
16. H. Ou, J. Lan, C.G. Armstrong, M.A. Price, An FE simulation and optimisation approach for the forging of aero-engine components, *J. Mater. Process. Technol.* 151(1-3) (2004) 208-216.
 17. J.L. Chenot, E. Massoni, Finite element modelling and control of new metal forming processes, *Int. J. Mach. Tools & Manuf.* 46 (2006) 1194–1200.
 18. B.A. Behrens, E. Doege, S. Reinsch, K. Telkamp, H. Daehndel, A. Specker, Precision forging processes for high-duty automotive components, *J. Mater. Process. Technol.* 185 (2007) 139–146.
 19. V. Ranatunga, J.S. Gunasekera, W.G. Frazier, Use of UBET for design of flash gap in closed die forging, *J. Mater. Process. Technol.* 111 (2001) 107-112.
 20. J. Hou, U. Stahlberg, Three-dimensional UBET model applied to the forging of square blocks between flat dies and grooved dies of simple geometry, *J. Mater. Process. Technol.* 62 (1996) 81-89.
 21. J. Mollar, L. Tran, D. Shrader, Augmented upper bound element technique for prediction of temperature and strain in forgings, *J. Mater. Process. Technol.* 152 (2004) 162-175.
 22. A.T. Male, M.G. Cockcroft, A method for the determination of the coefficient of friction of metals under condition of bulk plastic deformation, *J. Inst. Metals.* 93 (1964-65) 38-46.
 23. W. Johnson, P.B. Mellor, *Engineering Plasticity* 1st ed., Van-Nostrand Reinhold, New York, USA, 1973.